Journal of Reliability Science and Engineering

TOPICAL REVIEW • OPEN ACCESS

Dimension-reduction integration methods for uncertainty quantification of stochastic systems: a state-of-the-art review on moments estimation

To cite this article: Tao Wang *et al* 2025 *J. Reliab. Sci. Eng.* **1** 042001

View the article online for updates and enhancements.

You may also like

- On uniformly staggered testing strategy for redundant safety instrumented systems
Sun-Keun Seo and Won Young Yun
- Intelligent reliability assurance methodologies for engineering systems: advances and challenges
Zhiliang Liu, Qin Zhang, Yu Liu et al.
- A new Kalman filter algorithm based on the interval process model
Jinyang Li, Jinwu Li, Chengkai Shen et al.

This content was downloaded from IP address 118.123.172.214 on 15/12/2025 at 02:28

OPEN ACCESS
IOP Publishing | ISECAEP
Journal of Reliability Science and Engineering
J. Reliab. Sci. Eng. **1** (2025) 042001 (25pp)
https://doi.org/10.1088/3050-2454/ae1df9

Topical Review

Dimension-reduction integration methods for uncertainty quantification of stochastic systems: a state-of-the-art review on moments estimation

Tao Wang[1], **Da-Gang Lu**[2,*], **You Dong**[1,*], **Dan M Frangopol**[3] **and Yi-Qiu Tan**[4]

[1] Department of Civil and Environmental Engineering, The Hong Kong Polytechnic University, Hong Kong Special Administrative Region of China 999077, People's Republic of China
[2] School of Civil Engineering, Harbin Institute of Technology, Harbin, Heilongjiang 150090, People's Republic of China
[3] Department of Civil and Environmental Engineering, Engineering Research Center for Advanced Technology for Large Structural Systems (ATLSS Center), Lehigh University, Bethlehem, PA, United States of America
[4] School of Transportation Science and Engineering, Harbin Institute of Technology, Harbin, Heilongjiang 150090, People's Republic of China

E-mail: ludagang@hit.edu.cn, you.dong@polyu.edu.hk and pts-tao.wang@polyu.edu.hk

Received 15 July 2025, revised 20 October 2025
Accepted for publication 11 November 2025
Published 2 December 2025

Abstract

Estimating the moments of stochastic systems is a relatively common problem in engineering uncertainty quantification and reliability analysis. Dimension-reduction integration methods (DRIMs), derived from dimension-reduction models, provide the theoretical foundation for converting the high-dimensional integrals involved in stochastic system moment estimation into sets of low-dimensional integrals over component functions. These methods have emerged as important approaches for moment estimation. This paper provides a comprehensive review of existing DRIMs for stochastic system moment estimation, including a review of dimension-reduction models, DRIMs for moment estimation, and the combination of these integration methods with advanced numerical integration algorithms. Finally, the outlook and conclusion section identifies challenges and promising future research directions for DRIMs, thereby providing a foundational reference for researchers and practitioners in the field.

* Authors to whom any correspondence should be addressed.

Original content from this work may be used under the terms of the Creative Commons Attribution 4.0 licence. Any further distribution of this work must maintain attribution to the author(s) and the title of the work, journal citation and DOI.

© 2025 The Author(s). Published by IOP Publishing Ltd on behalf of the Institute of Systems Engineering, China Academy of Engineering Physics

Keywords: uncertainty quantification, statistical moments, dimension-reduction integration method, dimension-reduction model, multidimensional integration, stochastic mechanics

Nomenclature

Abbreviations

BDRM	Bivariate dimension-reduction model
BDRIM	Bivariate dimension-reduction integration method
CUT	Conjugate unscented transform
DRIMs	Dimension-reduction integration methods
ECUT	Enhanced conjugate unscented transform
GQR	Gaussian quadrature rules
GF-DRIM	Generalized factorized dimension-reduction integration method
H-DRM	Hybrid dimension-reduction model
HDMR	High dimensional model representation
HDRIM	Hybrid dimension-reduction integration method
HUT	High-order unscented transformation
MEM	Maximum entropy method
MCS	Monte Carlo simulation
M-UDRM	Multiplicative univariate dimension-reduction model
M-UDRIM	Multiplicative univariate dimension-reduction integration method
M-VDRIM	Multiplicative vector-based dimension-reduction integration method
M-BDRM	Multiplicative bivariate dimension-reduction model
M-BDRIM	Multiplicative bivariate dimension-reduction integration method
M-EDRM	Multiplicative exact dimension-reduction model
PDF	Probability density function
PNTT	Polynomial normal transformation technique
RDRIM	Reliability-based design optimization
RBDO	Refined dimension-reduction integration method
RDO	Robust design optimization
SPA	Saddle point approximation
SGI	Sparse grid integration
UDRM	Univariate dimension-reduction model
UDRIM	Univariate dimension-reduction integration method
UT	Unscented transformation
Va-DRMs	Variable-based dimension-reduction models
Ve-DRMs	Vector-based dimension-reduction models
VDRIM	Vector-based dimension-reduction integration method

Notations

$\boldsymbol{a}$	Multi-index vector
G	Input–output mapping
$G_i(\boldsymbol{\Theta}_{Si})$	Component function associated with $\boldsymbol{\Theta}_{Si}$
G_{con}	Constant term
G_i^{vec}	Component functions for $d_{\text{dim}} \leqslant 2$
G_i^{var}	Component functions represented by an un-truncated Va-DRM
$M_{Z,q}$	qth order raw moments
$m_{Z,q}$	qth central moments
m_i	Number of random variables in $\boldsymbol{\Theta}_{Si}$
m_j	Number of random variables in $\boldsymbol{\Theta}_{Sj}$
m_{GH}	Number of quadrature points
m_{CUT}	Number of abscissas for CUT methods
n_s	Dimension of numerical integration in HUT method
N_{dim}	Dimension of random input vector
p_v	Count of sub-vectors with $d_{\text{dim}} \leqslant 2$
s	Truncation order
u_{i,l_i}	Quadrature nodes in GQR
$\boldsymbol{u}_i^c$	Abscissas in CUT method
$\boldsymbol{u}_0^h$	Integration points in HUT method
$\underline{\boldsymbol{v}}_{i,Sc}$	Sub-vector of $\boldsymbol{\theta}_{Sc}$ excluding coordinate $\boldsymbol{\theta}_{Si,c}$
w_{i,l_i}	Weights in GQR
w_0^h	Weights in HUT method
w_i^c	Weighs in CUT methods
Z	System response
$\boldsymbol{\Theta}$	Random input vector
$\underline{\boldsymbol{\Theta}}_i$	Sub-vector of $\boldsymbol{\Theta}$ excluding Θ_i
Θ_i	Random variable
$\boldsymbol{\theta}_c$	Reference point
$\theta_t^{(k)}$	kth sample of Θ_t
$\underline{\boldsymbol{\theta}}_{i,c}$	Sub-vectors of $\boldsymbol{\theta}_c$ excluding the ith coordinate
$\underline{\boldsymbol{\theta}}_{i_1 i_2,c}$	Sub-vectors of $\boldsymbol{\theta}_c$ excluding the i_1th and i_2th coordinates
$\underline{\boldsymbol{\theta}}_{i_1 i_2 \ldots i_l,c}$	Sub-vectors of $\boldsymbol{\theta}_c$ excluding the corresponding coordinates of $\Theta_{i_1}, \Theta_{i_2}, \ldots, \Theta_{i_l}$
$\boldsymbol{\theta}_{Sc}$	Reference points of $\left(\boldsymbol{\Theta}_{S1}, \boldsymbol{\Theta}_{S2}, \ldots, \boldsymbol{\Theta}_{S_{p_t}}\right)$
$\boldsymbol{\theta}_{Si,c}$	Corresponding coordinates of $\boldsymbol{\Theta}_{Si}$
$\underline{\boldsymbol{\theta}}_{i,Sc}$	Reference points of $\boldsymbol{\Theta}_i$
$\Theta_{Si,a}$	ath variable of $\boldsymbol{\Theta}_{Si}$
$\Theta_{Sj,b}$	bth variable of $\boldsymbol{\Theta}_{Sj}$
$\boldsymbol{\Theta}_{Si}^{\text{vec}}$	Sub-vectors with dimension $d_{\text{dim}} \leqslant 2$
$\boldsymbol{\Theta}_{Si}^{\text{var}}$	Sub-vectors with dimension $d_{\text{dim}} \geqslant 3$
$\Omega_{\boldsymbol{\Theta}}$	Distribution domain of $\boldsymbol{\Theta}$
$\mathbb{E}(\cdot)$	Expectation
μ_Z	Mean
$p_{\Theta_i}(\theta_i)$	Marginal PDF of Θ_i
σ_Z	Standard deviation
γ_Z	Coefficient of skewness
k_Z	Coefficient of kurtosis
ε	A small positive real number
$Q_G(\Theta_{i_1}, \Theta_{i_2})$	Indicator function
σ_i, c_i^m, $s_i^{n_s}(h_s)$	Reference point sets in CUT methods
$\mathbf{N}_i^{\xi}(\Theta_i)$	Nodal coordinates of the ith-dimension at level for SGI
ξ	Non-negative integer signifying the precision level for SGI
$\otimes$	Tensor product operator
β	Number of exclusive subsets for SGI
ψ	Additional weight factor
$\eta(a_i)$	a sequence function

1. Introduction

In civil, mechanical, electrical, and other engineering disciplines, as well as in scientific disciplines such as applied mathematics and information science, systems are inherently subjected to various sources of uncertainty. These uncertainties stem from intrinsic physical randomness, such as manufacturing errors [1–6], geometric defects [7–9], and boundary constraints [10–14] and external excitations including hurricanes [15–18], earthquakes [19–21], and icing [22–25]). The propagation of these uncertainties through complex system models (e.g. nonlinear finite element analysis, computational fluid dynamics) leads to stochastic responses. Accurately quantifying response uncertainty is not an end in itself but a critical prerequisite for foundational tasks in reliability science and engineering, such as reliability analysis, risk assessment, and reliability/robust-based design optimization.

From a probabilistic perspective, the complete characterization of a stochastic response is given by its moments or PDF [26–29]. However, directly estimating the PDF for high-dimensional systems is often intractable. Consequently, statistical moments—including the mean (central tendency), variance (dispersion), skewness (asymmetry), and kurtosis (tail heaviness)—serve as fundamental proxies. They fulfill a dual role: firstly, they describe key distributional characteristics; secondly, they facilitate the reconstruction of the response PDF through techniques like the Pearson distribution families [30], SPA [31], PNTT [32], distribution reconstruction methods [33], MEM [34, 35], or iterative MEM [36, 37]. It is precisely this dual utility that makes the accurate and efficient estimation of moments a cornerstone of uncertainty quantification. Nevertheless, for high-dimensional systems lacking an explicit functional form, the computation of moments involves high-dimensional integrals, which confronts the notorious 'curse of dimensionality'. This renders traditional numerical quadrature infeasible and mandates computationally intensive simulations, making the development of efficient methods a pressing challenge.

To address this challenge, numerous efficient moment estimation methods have evolved into five primary paradigms: (1) *sampling-based methods* including (Crude MCS [38], Latin hypercube sampling [39]) and Quasi-MCS with low-discrepancy sequences [24, 40]; (2) *Bayesian integration methods* through probabilistic integration frameworks [41–43]; (3) *deterministic point-selection methods* encompassing point estimate methods [44–49], SGI [50–53], cubature rules [54, 55], UT [56–59], and CUT [60–63]; (4) *surrogate modeling-based methods* using metamodels [64, 65]; and (5) DRIMs [66–80]. While each paradigm has its merits, there remains a critical need for methods that are both theoretically rigorous and computationally efficient for high-dimensional integration.

Among these paradigms, DRIMs have emerged as a particularly powerful and theoretically grounded framework. DRIMs leverage dimension-reduction models to decompose a high-dimensional integral into a collection of lower-dimensional integrals, thereby effectively mitigating the curse of dimensionality. While several DRIMs have been proposed and successfully applied, *the literature lacks a unified framework that systematically categorizes these methods, elucidates their theoretical connections, and synthesizes their integration with advanced numerical schemes.* This gap hinders researchers and practitioners from gaining a holistic understanding and making informed choices.

To address this gap, this review provides a comprehensive and systematic examination of DRIMs for moment estimation. The specific contributions of this work are threefold:

(1) To establish a clear taxonomy of dimension-reduction models (variable-based, vector-based, and hybrid) and their corresponding integration methods and provide a critical analysis for DRIMs.
(2) To synthesize the integration of DRIMs with advanced numerical algorithms (e.g. HUT, CUT, SGI), highlighting synergistic advancements.
(3) To critically discuss persistent challenges and outline promising future research directions, thereby providing a roadmap for the continued evolution of this field.

The remainder of this paper is organized as follows: section 2 formally defines moments of random response functions. Section 3 categorizes and critically analyzes prevailing dimension-reduction models. Sections 4 and 5 synthesize DRIMs and their methodological enhancements for stochastic system moment estimation. Finally, sections 6 and 7 discuss emerging research trajectories and presents concluding insights on DRIM advancements.

2. Definition of response function moments

For general moments estimation problems, the mapping relationship between a N_{dim}-dimensional random input vector $\boldsymbol{\Theta} = [\Theta_1, \Theta_2, \ldots, \Theta_{N_{\text{dim}}}]^{\mathrm{T}}$ and the system response Z is defined as:

$$Z = G(\boldsymbol{\Theta}) \tag{1}$$

in which G: $\mathbb{R}^{N_{\text{dim}}} \to \mathbb{R}$ represents the input–output mapping.

The qth order raw moments $M_{Z,q}$ and central moments $m_{Z,q}$ of Z are respectively given by:

$$\begin{cases} M_{Z,q} = \mathbb{E}\left[Z^q\right] = \displaystyle\int_{\Omega_\Theta} \left[G(\boldsymbol{\theta})\right]^q p_{\boldsymbol{\Theta}}(\boldsymbol{\theta})\,\mathrm{d}\boldsymbol{\theta} \\ m_{Z,q} = \mathbb{E}\left[(Z-\mu_Z)^q\right] = \displaystyle\int_{\Omega_\Theta} \left[G(\boldsymbol{\theta})-\mu_Z\right]^q p_{\boldsymbol{\Theta}}(\boldsymbol{\theta})\,\mathrm{d}\boldsymbol{\theta} \end{cases} \tag{2}$$

in which $\Omega_{\boldsymbol{\Theta}}$ denotes the distribution domain of $\boldsymbol{\Theta}$; $p_{\boldsymbol{\Theta}}(\boldsymbol{\theta})$ is the joint PDF of $\boldsymbol{\Theta}$; $E(\cdot)$ denotes the expectation and $\mu_Z = \mathbb{E}[Z]$ is the mean.

When components of $\boldsymbol{\Theta}$ are mutually independent, the joint PDF factorizes as:

$$p_{\boldsymbol{\Theta}}(\boldsymbol{\theta}) = \prod_{i=1}^{N_{\text{dim}}} p_{\Theta_i}(\theta_i) \tag{3}$$

where $p_{\Theta_i}(\theta_i)$ is the marginal PDF of Θ_i.

The conversion between the first l raw moments $M_{Z,q}$ and central moments $m_{Z,q}$ of Z is governed by the binomial expansion:

$$m_{Z,q} = \sum_{k=0}^{q} \binom{q}{k} (-1)^{q-k} M_{Z,k} (\mu_Z)^{q-k}, q \leqslant l. \tag{4}$$

Key statistical descriptors derived from the first four raw or central moments include:

Mean: $\mu_Z = M_{Z,1}$

Standard deviation: $\sigma_Z = \sqrt{m_{Z,2}} = \sqrt{M_{Z,2} - M_{Z,1}^2}$

Coefficient of Skewness:

$$\gamma_Z = \frac{m_{Z,3}}{\sigma_Z^3} = \frac{M_{Z,3} - 3M_{Z,2}M_{Z,1} + 2M_{Z,1}^3}{\sigma_Z^3} \tag{5}$$

Coefficient of Kurtosis:

$$k_Z = \frac{m_{Z,4}}{\sigma_Z^4} = \frac{M_{Z,4} - 4M_{Z,3}M_{Z,1} + 6M_{Z,2}M_{Z,1}^2 - 3M_{Z,1}^4}{\sigma_Z^4}.$$

3. Categorization and review of dimension-reduction models

As the theoretical foundation for DRIMs, this section categorizes and synthesizes existing dimension-reduction models used to characterize system response functions $Z = G(\boldsymbol{\Theta})$, comprising three classes: (1) Va-DRMs, (2) Ve-DRMs, and (3) H-DRM containing both variables and vectors.

3.1. Va-DRMs

Va-DRMs approximate high-dimensional response functions $Z = G(\boldsymbol{\Theta})$ using low-order component functions that depend on reduced subsets of input variables, with both additive and multiplicative formulations available. Specifically, additive Va-DRMs, derived from HDMR [81–83], express the response function as a summation of component functions:

$$\begin{aligned} Z = G(\boldsymbol{\Theta}) = G_0 &+ \sum_i G_i(\Theta_i) + \sum_{i_1 < i_2 \leqslant N_{\text{dim}}} G_{i_1 i_2}(\Theta_{i_1}, \Theta_{i_2}) \\ &+ \ldots + \sum_{i_1 < i_2 < \ldots < i_l \leqslant N_{\text{dim}}} G_{i_1 i_2 \ldots i_l}(\Theta_{i_1}, \Theta_{i_2}, \ldots, \Theta_{i_l}) \\ &+ \ldots + G_{1,2,\ldots,N_{\text{dim}}}(\Theta_1, \Theta_2, \ldots, \Theta_{N_{\text{dim}}}) \end{aligned} \tag{6}$$

in which

$$\begin{cases} G_0 = G(\boldsymbol{\theta}_c) \\ G_i(\Theta_i) = G\left(\Theta_i, \underline{\boldsymbol{\theta}}_{i,c}\right) - G_0 \\ G_{i_1 i_2}(\Theta_{i_1}, \Theta_{i_2}) = G\left(\Theta_{i_1}, \Theta_{i_2}, \underline{\boldsymbol{\theta}}_{i_1 i_2, c}\right) - G_{i_1}(\Theta_{i_1}) \\ \quad - G_{i_2}(\Theta_{i_2}) - G_0 \\ \qquad \vdots \\ G_{i_1 i_2 \cdots i_l}(\Theta_{i_1}, \Theta_{i_2}, \cdots, \Theta_{i_l}) = G\left(\Theta_{i_1}, \Theta_{i_2}, \cdots, \Theta_{i_l}, \underline{\boldsymbol{\theta}}_{i_1 i_2 \cdots i_l, c}\right) \\ \qquad - \sum_{\{j_1 j_2 \cdots j_{l-1}\} \subset \{i_1 i_2 \cdots i_l\}} G_{j_1 j_2 \cdots j_{l-1}}\left(\Theta_{j_1}, \Theta_{j_2}, \cdots, \Theta_{j_{l-1}}\right) \\ \qquad - \sum_{\{j_1 j_2 \cdots j_{l-2}\} \subset \{i_1 i_2 \cdots i_l\}} G_{j_1 j_2 \cdots j_{l-2}}\left(\Theta_{j_1}, \Theta_{j_2}, \cdots, \Theta_{j_{l-2}}\right) \\ \qquad - \cdots - \sum_{j \subset \{i_1 i_2 \cdots i_l\}} G_j(\Theta_j) - G_0 \end{cases} \tag{7}$$

where $\boldsymbol{\theta}_c = \left(\theta_{c,1}, \theta_{c,2}, \ldots, \theta_{c,N_{\text{dim}}}\right)$ denotes the reference point, $\underline{\boldsymbol{\theta}}_{i,c}$ denotes sub-vectors of $\boldsymbol{\theta}_c$ excluding the ith coordinate, $\underline{\boldsymbol{\theta}}_{i_1 i_2, c}$ is sub-vectors of $\boldsymbol{\theta}_c$ excluding the i_1th and i_2th coordinates, $\underline{\boldsymbol{\theta}}_{i_1 i_2 \ldots i_l, c}$ is sub-vectors of $\boldsymbol{\theta}_c$ excluding the corresponding coordinates of $\Theta_{i_1}, \Theta_{i_2}, \ldots, \Theta_{i_l}$.

When the truncation order is set to s, the system response Z can be characterized as:

$$\begin{aligned} Z &\approx G^{(s-\text{HDMR})}(\boldsymbol{\Theta}) \\ &= G_0 + \sum_i G_i(\Theta_i) + \sum_{1 \leqslant i_1 < i_2 \leqslant N_{\text{dim}}} G_{i_1 i_2}(\Theta_{i_1}, \Theta_{i_2}) \\ &\quad + \cdots + \sum_{i_1 < i_2 < \cdots < i_s} G_{i_1 i_2 \cdots i_s}(\Theta_{i_1}, \Theta_{i_2}, \cdots, \Theta_{i_s}). \end{aligned} \tag{8}$$

Moreover, an equivalent formulation to equation (8) was established by Xu and Rahman [67], expressed as:

$$\begin{aligned} Z = G(\boldsymbol{\Theta}) \approx \sum_{r=0}^{s} (-1)^r \begin{pmatrix} N_{\text{dim}} - s + r - 1 \\ r \end{pmatrix} \\ \times \sum_{i_1 < i_2 < \ldots < i_{s-r}} G\left(\Theta_{i_1}, \Theta_{i_2}, \ldots, \Theta_{i_{s-r}}, \underline{\boldsymbol{\theta}}_{i_1 i_2 \ldots i_{s-r}, c}\right). \end{aligned} \tag{9}$$

Multiplicative Va-DRMs originate from either factorized high-dimensional model representation [84, 85] or multiplicative dimension-reduction model [86, 87]. The s-variate truncated multiplicative form can be expressed as [36]

$$Z \approx r_0 \left[\prod_{i=1}^{N_{\text{dim}}} (1 + r_i(\Theta_i))\right] \left[\prod_{\substack{i_i, i_2 = 1 \\ i_1 < i_2}}^{N_{\text{dim}}} (1 + r_{i_1 i_2}(\Theta_{i_1}, \Theta_{i_2}))\right] \times \cdots \times \left[\prod_{i_1 < i_2 < \cdots < i_s} (1 + r_{i_1 i_2 \cdots i_s}(\Theta_{i_1}, \Theta_{i_2}, \cdots, \Theta_{i_s}))\right] \tag{10}$$

in which

$$\begin{cases} r_0 = G_0 = G(\boldsymbol{\theta}_c) \\ r_i(\Theta_i) = \dfrac{G(\Theta_i, \underline{\boldsymbol{\theta}}_{i,c})}{G_0} - 1 \\ r_{i_1 i_2}(\Theta_{i_1}, \Theta_{i_2}) = \dfrac{G_0 G(\Theta_{i_1}, \Theta_{i_2}, \underline{\boldsymbol{\theta}}_{i_1 i_2, c})}{G(\Theta_{i_1}, \underline{\boldsymbol{\theta}}_{i_1, c}) G(\Theta_{i_2}, \underline{\boldsymbol{\theta}}_{i_2, c})} - 1 \\ \vdots \end{cases}. \tag{11}$$

Remarkably, an equivalent formulation to equations (10) and (11) was derived in [87]:

$$\begin{aligned} Z &= G(\boldsymbol{\Theta}) \\ &\approx \frac{\displaystyle\prod_{\substack{k_1 = s, s-2, \\ s-4, \ldots}} \left\{ \left[\prod_{\substack{1 \leqslant i_1 < i_2 < \cdots \\ < i_{k_1} \leqslant N_{\text{dim}}}} G\left(\theta_{i_1}, \theta_{i_2}, \ldots, \theta_{i_{k_1}}, \underline{\boldsymbol{\theta}}_{i_1 i_2 \cdots i_{k_1}, c}\right) \right]^{\binom{N_{\text{dim}} - k_1 - 1}{s_1 - k}} \right\}}{\displaystyle\prod_{\substack{k_2 = s-1, s-3, \\ s-5, \ldots}} \left\{ \left[\prod_{\substack{1 \leqslant j_1 < j_2 < \cdots \\ < j_{k_2} \leqslant N_{\text{dim}}}} G\left(\theta_{j_1}, \theta_{j_2}, \ldots, \theta_{j_{k_2}}, \underline{\boldsymbol{\theta}}_{j_1 j_2 \cdots j_{k_2}, c}\right) \right]^{\binom{N_{\text{dim}} - k_2 - 1}{s_2 - k}} \right\}}. \end{aligned} \tag{12}$$

For practical implementation of additive or multiplicative Va-DRMs, the truncation order is commonly set to $s = 1$ or 2, yielding the following simplified representations:

- Additive

$$\begin{aligned} Z &= G(\boldsymbol{\Theta}) \\ &\approx \begin{cases} \displaystyle\sum_{i=1}^{N_{\text{dim}}} G(\Theta_i, \underline{\boldsymbol{\theta}}_{i,c}) - (N_{\text{dim}} - 1) G(\boldsymbol{\theta}_c), \text{for } s = 1; \\ \displaystyle\sum_{i_1 < i_2} G(\Theta_{i_1}, \Theta_{i_2}, \underline{\boldsymbol{\theta}}_{i_1 i_2, c}) - (N_{\text{dim}} - 2) \sum_{i=1}^{N_{\text{dim}}} G(\Theta_i, \underline{\boldsymbol{\theta}}_{i,c}) \\ \quad + \dfrac{N_{\text{dim}}^2 - 3N_{\text{dim}} + 2}{2} G(\boldsymbol{\theta}_c), \text{for } s = 2. \end{cases} \end{aligned} \tag{13}$$

- Multiplicative

$$\begin{aligned} Z &= G(\boldsymbol{\Theta}) \\ &\approx \begin{cases} [G(\boldsymbol{\theta}_c)]^{1 - N_{\text{dim}}} \displaystyle\prod_{i=1}^{N_{\text{dim}}} G(\Theta_i, \underline{\boldsymbol{\theta}}_{i,c}), \text{for } s = 1; \\ \dfrac{[G(\boldsymbol{\theta}_c)]^{\frac{(N_{\text{dim}} - 1)(N_{\text{dim}} - 2)}{2}} \displaystyle\prod_{1 \leqslant i_1 < i_2 \leqslant N_{\text{dim}}} G(\Theta_{i_1}, \Theta_{i_2}, \underline{\boldsymbol{\theta}}_{i_1 i_2, c})}{\left[\displaystyle\prod_{i=1}^{N_{\text{dim}}} G(\Theta_i, \underline{\boldsymbol{\theta}}_{i,c})\right]^{N_{\text{dim}} - 2}}, \\ \text{for } s = 2 \end{cases} \end{aligned} \tag{14}$$

For these equations, the $s = 1$ case corresponds to the UDRM [66] for equation (13) and the M-UDRM [86] for equation (14). Similarly, the $s = 2$ case yields the BDRM [67] for equation (13) and the M-BDRM [87] for equation (14).

3.2. Ve-DRMs

Ve-DRMs, derived through the vector classification approach [37, 88], represent the response function via component functions corresponding to sub-vectors. The vector classification process first identifies interaction terms Θ_{i_1} and Θ_{i_2} in $G(\boldsymbol{\Theta})$ through the following procedure:

$$\frac{\left|\begin{array}{l}\left[G\left(\theta_{i_1}^{(2)},\theta_{i_2}^{(1)},\underline{\boldsymbol{\theta}}_{i_1i_2,c}\right)-G\left(\theta_{i_1}^{(1)},\theta_{i_2}^{(1)},\underline{\boldsymbol{\theta}}_{i_1i_2,c}\right)\right]\\ -\left[G\left(\theta_{i_1}^{(2)},\theta_{i_2}^{(2)},\underline{\boldsymbol{\theta}}_{i_1i_2,c}\right)-G\left(\theta_{i_1}^{(1)},\theta_{i_2}^{(2)},\underline{\boldsymbol{\theta}}_{i_1i_2,c}\right)\right]\end{array}\right|}{\min\left\{\left|\left[G\left(\theta_{i_1}^{(2)},\theta_{i_2}^{(1)},\underline{\boldsymbol{\theta}}_{i_1i_2,c}\right)-G\left(\theta_{i_1}^{(1)},\theta_{i_2}^{(1)},\underline{\boldsymbol{\theta}}_{i_1i_2,c}\right)\right]\right|,\left|\left[G\left(\theta_{i_1}^{(2)},\theta_{i_2}^{(2)},\underline{\boldsymbol{\theta}}_{i_1i_2,c}\right)-G\left(\theta_{i_1}^{(1)},\theta_{i_2}^{(2)},\underline{\boldsymbol{\theta}}_{i_1i_2,c}\right)\right]\right|\right\}}\geqslant\varepsilon \tag{15}$$

where $\theta_t^{(k)}$ ($k=1,2$ and $t=i,j$) denotes the kth sample of Θ_t, ε represents a small positive real number. Subsequently, the indicator function $Q_G(\Theta_{i_1},\Theta_{i_2})$ quantifying interactions between Θ_{i_1} and Θ_{i_2} is defined as

$$Q_G(\Theta_{i_1},\Theta_{i_2})=\begin{cases}1, \text{ if cross terms of } \Theta_{i_1} \text{and } \Theta_{i_2} \text{ exist}\\ 0, \text{ otherwise}\end{cases}. \tag{16}$$

Using equation (16), we verify whether the condition in equation (17) is satisfied. If satisfied, $\boldsymbol{\Theta}_{Si}$ and $\boldsymbol{\Theta}_{Sj}$ can be partitioned into independent sub-vectors:

$$\sum_{a=1}^{m_i}\sum_{b=1}^{m_j}Q_G(\Theta_{Si,a},\Theta_{Sj,b})=0 \tag{17}$$

where $\Theta_{Si,a}$ and $\Theta_{Sj,b}$ denotes the ath variable of $\boldsymbol{\Theta}_{Si}$ and the bth variable of $\boldsymbol{\Theta}_{Sj}$, respectively, and m_i (or m_j) represents the number of random variables in $\boldsymbol{\Theta}_{Si}$ (or $\boldsymbol{\Theta}_{Sj}$). Through this process, the original vector $\boldsymbol{\Theta}$ in $G(\boldsymbol{\Theta})$ decomposes into p_t sub-vectors, i.e. $\boldsymbol{\Theta}_{S1},\boldsymbol{\Theta}_{S2},\ldots,\boldsymbol{\Theta}_{S_{p_t}}$, satisfying

$$Q_G(\boldsymbol{\Theta}_{Si},\boldsymbol{\Theta}_{Sj})=0\ ,\ i,j=1,2,\cdots,p_t \text{ and } i\neq j \tag{18}$$

where p_t denotes the number of sub-vectors.

The system response Z is then characterized by the superposition of component functions corresponding to these sub-vectors [63, 88], i.e.

$$Z=G(\boldsymbol{\Theta})=\sum_{i=1}^{p_t}G_i(\boldsymbol{\Theta}_{Si})+(1-p_t)\,G(\boldsymbol{\theta}_{Sc}) \tag{19}$$

in which $\boldsymbol{\theta}_{Sc}=(\boldsymbol{\theta}_{S1,c},\boldsymbol{\theta}_{S2,c},\ldots,\boldsymbol{\theta}_{Spt,c})$ denotes the reference points of $(\boldsymbol{\Theta}_{S1},\boldsymbol{\Theta}_{S2},\ldots,\boldsymbol{\Theta}_{S_{p_t}})$ and $\boldsymbol{\theta}_{Si,c}$ represents the corresponding coordinates of $\boldsymbol{\Theta}_{Si}$; $G_i(\boldsymbol{\Theta}_{Si})=G(\boldsymbol{\theta}_{S1,c},\ldots,\boldsymbol{\theta}_{S(i-1),c},\boldsymbol{\Theta}_{Si},\boldsymbol{\theta}_{S(i+1),c},\ldots,\boldsymbol{\theta}_{S_{p_t},c})$ is the component function associated with $\boldsymbol{\Theta}_{Si}$.

Notably, analogous to the additive approach, Wang *et al* [37] proposed the multiplicative vector-based dimension-reduction model, also termed the M-EDRM:

$$Z=G(\boldsymbol{\Theta})=G(\boldsymbol{\theta}_{Sc})^{(1-p_t)}\prod_{i=1}^{p_t}G_i(\boldsymbol{\Theta}_{Si}) \tag{20}$$

where a nonlinear transformation ensures positivity of the response function. As this model primarily serves fractional moments estimation for structural reliability analysis [37], its detailed theoretical derivation is beyond this paper's scope.

3.3. H-DRM

The H-DRM, incorporating component functions for both individual variables and sub-vectors, is also termed the refined dimension-reduction model and was established by Wang *et al* [89]. This model decomposes the response as:

$$\begin{aligned}Z=G(\boldsymbol{\Theta})=&\underbrace{\sum_{i=1}^{p_v}G_i(\boldsymbol{\Theta}_{Si}^{\text{vec}})}_{\substack{\text{Component function of}\\ \text{random vectors}\,(d_{\text{dim}}\leqslant 2)}}\\ &+\underbrace{\sum_{i=1}^{p_t-p_v}G_i\left(\Theta_{i_1},\Theta_{i_2},\cdots,\Theta_{i_{d_{\text{dim}}}},\underline{\boldsymbol{v}}_{i,Sc}\right)}_{\substack{\text{Component function of}\\ \text{random variables}\,(d_{\text{dim}}\geqslant 3)}}+\underbrace{(1-p_t)\,G(\boldsymbol{\theta}_{Sc})}_{\text{Constant term}}\\ \triangleq&\sum_{i=1}^{p_v}G_i^{\text{vec}}+\sum_{i=1}^{p_t-p_v}G_i^{\text{var}}+G_{\text{con}}\end{aligned} \tag{21}$$

$$\begin{aligned}G_i^{\text{var}}&=G_i\left(\Theta_{i_1},\Theta_{i_2},\cdots,\Theta_{i_{d_{\text{dim}}}},\underline{\boldsymbol{v}}_{i,Sc}\right)\\ &=\sum_{r=0}^{s}(-1)^r\binom{d_{\text{dim}}-s+r-1}{r}\sum_{i_1<i_2<\ldots<i_{s-r}}\\ &\quad G\left(\Theta_{i_1},\Theta_{i_2},\ldots,\Theta_{i_{s-r}},\underline{\boldsymbol{\theta}}_{i_1i_2\ldots i_{s-r},c},\underline{\boldsymbol{v}}_{i,Sc}\right)\end{aligned} \tag{22}$$

in which $\underline{\boldsymbol{v}}_{i,Sc}$ represents a sub-vector of $\boldsymbol{\theta}_{Sc}$ excluding coordinate $\boldsymbol{\theta}_{Si,c}$; $\boldsymbol{\Theta}_{Si}^{\text{vec}}$ and $\boldsymbol{\Theta}_{Si}^{\text{var}}$ represent sub-vectors with dimension $d_{\text{dim}}\leqslant 2$ and $d_{\text{dim}}\geqslant 3$ respectively; p_v is the count of sub-vectors with $d_{\text{dim}}\leqslant 2$; G_{con} denotes constant term; G_i^{vec} denotes the component functions for $d_{\text{dim}}\leqslant 2$; G_i^{var} is the component functions represented by an un-truncated Va-DRM when $s=d_{\text{dim}}$.

For high-dimensional sub-vectors, further truncation to order $s<d_{\text{dim}}$ is required. This necessitates a generalized interaction indicator $Q_G(\Theta_{i_1},\Theta_{i_2},\cdots,\Theta_{i_l})$ for the interaction terms of $\Theta_{i_1},\Theta_{i_2},\cdots,\Theta_{i_l}$ [89]

$$\begin{aligned}Q_G(\Theta_{i_1},\Theta_{i_2},\cdots,\Theta_{i_l})&=\prod_{1<k<m<l}Q_G(\Theta_{i_k},\Theta_{i_m})\\ &=\begin{cases}1, \text{ if the cross terms of } \Theta_{i_k} \text{ and } \Theta_{i_m} \text{ exist}\\ 0, \text{ otherwise}\end{cases}.\end{aligned} \tag{23}$$

Table 1. Comparative summary of dimension-reduction models.

Model category	Key advantage	Primary limitation	Ideal use-case
Additive Va-DRMs	High computational efficiency; general applicability	Large truncation error for strong/high-order interactions	High-dimensional screening; systems with weak additive interactions
Multiplicative Va-DRMs	High accuracy/efficiency for multiplicative systems & positive-valued responses	Not directly suitable for non-positive responses	Systems with multiplicative interactions.
Ve-DRMs	High accuracy by preserving interaction structure between sub-vectors	Computational cost can be high if sub-vectors are high-dimensional	Systems decomposable into independent, low-dimensional subsystems
H-DRM	Optimal balance for complex systems; versatile and robust	Highest implementation complexity	Systems with mixed interaction strengths (strong localized and weak global effects)

By integrating equation (22) with equation (23), unnecessary interaction terms in G_i^{var} can be further eliminated. Crucially, this identification incurs no additional computational cost, as equation (23) directly utilizes results from the vector classification phase.

The H-DRM synergistically integrates the advantages of Va-DRMs and Ve-DRMs through a two-stage dimension-reduction framework: (1) precise component representation via vector classification; (2) secondary dimension reduction of moderately/high-dimensional component functions using additive Va-DRMs. This dual-phase approach minimizes truncation error by preserving low-dimensional vectors and retaining statistically significant variables. Consequently, the H-DRM simultaneously addresses two critical limitations: (1) large truncation errors in Va-DRMs (particularly additive forms) for strongly interacting systems; (2) computational inefficiency in Ve-DRMs when handling high-dimensional component functions.

3.4. Comparative analysis: advantages and limitations

The choice of an appropriate dimension-reduction model is pivotal for balancing computational efficiency and estimation accuracy in engineering applications. This section provides a comparative analysis of the three categories of models, with their key characteristics summarized in table 1.

Va-DRMs, particularly in their *additive form* with low truncation orders ($s = 1, 2$), are celebrated for their remarkable computational efficiency, which makes them feasible for very high-dimensional problems. The primary limitation of Va-DRMs is their inability to *fully capture strong interaction effects* among input variables beyond the specified truncation order. For instance, UDRM ($s = 1$) completely neglects all interactions, which can lead to significant truncation errors for systems with pronounced coupling or nonlinear interactions. While BDRM ($s = 2$) can capture pairwise interactions, it may still be insufficient for systems governed by higher-order interactions. Consequently, additive Va-DRMs are best suited for problems with weak to moderate interactions or as a highly efficient first approximation.

Multiplicative Va-DRMs (e.g. M-UDRM, M-BDRM) offer a significant advantage for a specific class of problems: they provide a more natural and compact representation for *systems with inherent multiplicative interactions or positive-valued responses*. This makes them highly efficient for fractional moment estimation, which is crucial for reliability analysis. Their principal limitation is the requirement for a strictly positive response function, as negative values necessitate nonlinear transformations that can compromise accuracy.

Ve-DRMs address the core limitation of Va-DRMs by explicitly identifying and grouping interacting variables into sub-vectors through the vector classification process. This allows them to *precisely characterize the true interaction structure of the system*, effectively eliminating truncation error associated with unaccounted high-order interactions between sub-vectors. This makes Ve-DRMs highly accurate for systems with known or identifiable clustered interactions. The main drawback is their computational dependency on the outcome of the vector classification. If the decomposition results in one or several high-dimensional sub-vectors, the computational cost for evaluating these components can become prohibitive. Thus, Ve-DRMs are most powerful when the system naturally decomposes into low-dimensional, weakly interacting sub-systems.

The H-DRM was developed specifically to synergize the strengths of aforementioned models while mitigating their weaknesses. It leverages the precision of vector classification to preserve low-dimensional interacting groups (dimension $\leqslant 2$) but applies a secondary *variable-based decomposition* to any remaining high-dimensional sub-vectors. This two-stage approach optimally balances accuracy and efficiency. It *minimizes truncation error* by retaining significant low-dimensional interactions in their exact form, while simultaneously controlling computational cost by breaking down high-dimensional components. The trade-off is an increase in conceptual and implementation complexity compared to the simpler Va-DRMs. The H-DRM is particularly well-suited for complex systems that exhibit a mix of strong localized interactions within clusters and a larger set of weakly interacting variables.

4. Review of DRIMs for moments estimation

This section reviews three categories of DRIMs for moments estimation, consistent with the classification of

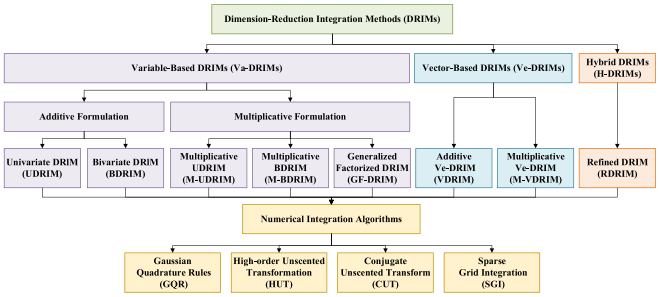


Figure 1. A flowchart illustrating the classification of DRIMs for moment estimation in stochastic systems.

dimension-reduction models in previous section: Va-DRMs-based, Ve-DRMs-based, and H-DRM-based DRIMs. A flowchart illustrating the classification of DRIMs for moment estimation in stochastic systems can be discovered in figure 1. It is necessary to clarify that the DRIMs discussed in following sections are formulated under the foundational assumption that the components of the input random vector $\boldsymbol{\Theta} = [\Theta_1, \Theta_2, \ldots, \Theta_{N_{\text{dim}}}]^{\text{T}}$ are mutually independent Gaussian distribution random variables. For problems involving dependent random inputs or non-Gaussian distribution random variables, transformations such as the Rosenblatt transformation [90], Nataf transformation [91] or generalized Nataf transformation [92] map them to standard Gaussian variates.

4.1. Va-DRMs-based DRIMs

The mean μ_Z and the qth central moments $m_{Z,q}$ of the system response Z are derived from s-order truncated additive Va-DRMs as [67]

$$\mu_Z \approx \sum_{k=0}^{s} (-1)^i \begin{pmatrix} N_{\text{dim}} - s + k - 1 \\ k \end{pmatrix} \sum_{i_1<i_2<i_3\ldots<i_{s-k}} \mathbb{E}\left[G\left(\Theta_{i_1}, \Theta_{i_2}, \ldots, \Theta_{i_{s-k}}, \underline{\boldsymbol{\theta}}_{i_1 i_2 \ldots i_{s-k}, c}\right)\right] \tag{24}$$

$$m_{Z,q} \approx \sum_{k=0}^{s} (-1)^i \begin{pmatrix} N_{\text{dim}} - s + k - 1 \\ k \end{pmatrix} \sum_{i_1<i_2<i_3\ldots<i_{s-k}} \times \mathbb{E}\left[\left(G\left(\Theta_{i_1}, \Theta_{i_2}, \ldots, \Theta_{i_{s-k}}, \underline{\boldsymbol{\theta}}_{i_1 i_2 \ldots i_{s-k}, c}\right) - \mu_Z\right)^q\right]. \tag{25}$$

For practical applications, the truncation order is typically limited to $s = 1$ or $s = 2$, corresponding to the UDRM and BDRM. Using the UDRM ($s = 1$), the moments of Z are derived as follows [66]

$$\mu_Z \approx \sum_{i=1}^{N_{\text{dim}}} \mathbb{E}\left(G\left(\Theta_i, \underline{\boldsymbol{\theta}}_{i,c}\right)\right) - (N_{\text{dim}} - 1)\, G(\boldsymbol{\theta}_c) \tag{26}$$

$$m_{Z,q} \approx \mathbb{E}\left[\left(\sum_{i=1}^{N_{\text{dim}}} G\left(\Theta_i, \underline{\boldsymbol{\theta}}_{i,c}\right) - (N_{\text{dim}} - 1)\, G(\boldsymbol{\theta}_c) - \mu_Z\right)^q\right] = \sum_{i=0}^{q} \begin{pmatrix} q \\ i \end{pmatrix} s_n^i [-(N_{\text{dim}} - 1)\, G(\boldsymbol{\theta}_c) - \mu_Z]^{q-i} \tag{27}$$

in which $s^i{}_n$ and its initial value are defined by the following recursive relation:

$$\begin{aligned} s_n^i &= \sum_{k=0}^{i} \begin{pmatrix} i \\ k \end{pmatrix} s_{n-1}^k \mathbb{E}\left[G^{i-k}(\theta_{1,c}, \theta_{2,c}, \ldots, \Theta_n)\right], \\ s_1^i &= \mathbb{E}\left[G^i(\Theta_1, \theta_{2,c}, \ldots, \theta_{n,c})\right], i = 0, \ldots, q. \end{aligned} \tag{28}$$

Notably, equations (26)–(28) require solely one-dimensional integrals that can be evaluated using GQR. This computational framework constitutes the UDRIM.

The moments of Z are derived from the BDRM as follows [93],

$$\mu_Z \approx \sum_{i<j} \mathbb{E}\left[G\left(\Theta_i, \Theta_j, \underline{\boldsymbol{\theta}}_{ij,c}\right)\right] - (N_{\text{dim}} - 2) \sum_{k=1}^{N_{\text{dim}}} \times \mathbb{E}\left[G\left(\Theta_k, \underline{\boldsymbol{\theta}}_{k,c}\right)\right] + \frac{(N_{\text{dim}} - 1)(N_{\text{dim}} - 2)}{2} G(\boldsymbol{\theta}_c) \tag{29}$$

$$m_{Z,q} \approx \sum_{i<j} \mathbb{E}\left[\left(G\left(\Theta_i, \Theta_j, \underline{\boldsymbol{\theta}}_{ij,c}\right) - \mu_Z\right)^q\right] - (N_{\text{dim}} - 2) \sum_{k=1}^{N_{\text{dim}}} \mathbb{E}\left[\left(G\left(\Theta_k, \underline{\boldsymbol{\theta}}_{k,c}\right) - \mu_Z\right)^q\right] + \frac{(N_{\text{dim}} - 1)(N_{\text{dim}} - 2)}{2} (G(\boldsymbol{\theta}_c) - \mu_Z)^q. \tag{30}$$

If the interaction terms of Θ_i and Θ_j are identified as 0, i.e. $Q_G(\Theta_i, \Theta_j) = 0$, $\mathbb{E}\left[G\left(\Theta_i, \Theta_j, \underline{\boldsymbol{\theta}}_{ij,c}\right)\right]$ and $\mathbb{E}\left[\left(G\left(\Theta_i, \Theta_j, \underline{\boldsymbol{\theta}}_{ij,c}\right) - \mu_Z\right)^q\right]$ in equations (29) and (30) become [94],

$$\mathbb{E}\left[G\left(\Theta_i, \Theta_j, \underline{\boldsymbol{\theta}}_{ij,c}\right)\right] = \mathbb{E}\left[G\left(\Theta_i, \underline{\boldsymbol{\theta}}_{i,c}\right) + G\left(\Theta_j, \underline{\boldsymbol{\theta}}_{j,c}\right) - G(\boldsymbol{\theta}_c)\right] \tag{31}$$

$$\mathbb{E}\left[\left(G\left(\Theta_i, \Theta_j, \underline{\boldsymbol{\theta}}_{ij,c}\right) - \mu_Z\right)^q\right] = \sum_{k_1+k_2+k_3=q} \frac{q!}{k_1! k_2! k_3!} (\mu_Z - G(\boldsymbol{\theta}_c))^{k_3} \times \mathbb{E}\left[\left(G\left(\Theta_i, \underline{\boldsymbol{\theta}}_{i,c}\right) - \mu_Z\right)^{k_1}\right] \times \mathbb{E}\left[\left(G\left(\Theta_j, \underline{\boldsymbol{\theta}}_{j,c}\right) - \mu_Z\right)^{k_2}\right]. \tag{32}$$

Subsequently, the expectation operators acting on functions in equations (29)–(32) are evaluated using the following expressions:

$$\begin{cases} \mathbb{E}\left[\left(G\left(\Theta_i,\underline{\boldsymbol{\theta}}_{i,c}\right)-\mu_Z\right)^m\right]=\sum\limits_{l_1=1}^{m_{\mathrm{GH}}} w_{1,l_1}\left(G\left(u_{1,l_1},\underline{\boldsymbol{\theta}}_{i,c}\right)-\mu_Z\right)^m \\ \mathbb{E}\left[\left(G\left(\Theta_i,\Theta_j,\underline{\boldsymbol{\theta}}_{ij,c}\right)-\mu_Z\right)^m\right]=\sum\limits_{l_1=1}^{m_{\mathrm{GH}}}\sum\limits_{l_2=1}^{m_{\mathrm{GH}}} w_{1,l_1}w_{2,l_2} \\ \left(G\left(u_{1,l_1},u_{2,l_2},\underline{\boldsymbol{\theta}}_{ij,c}\right)-\mu_Z\right)^m,\ m=k_i,q \end{cases} \tag{33}$$

where the quadrature nodes u_{i,l_i} and weights w_{i,l_i} are determined via GQR for the standard Gaussian random variables, m_{GH} is the number of quadrature points. To facilitate the description, we designate equations (29), (30) and (33) as the BDRIM, while equations (29)–(33) constitute the adaptive BDRIM. The choice of the truncation order s is critical in practical applications of Va-DRIMs, as it directly governs the trade-off between computational cost and estimation accuracy. While lower orders (s = 1,2) are most common, a principled strategy for selection enhances methodological robustness. The following guidelines are proposed: (i) default to univariate decomposition (s = 1): for initial analysis where the response function is suspected to be weakly nonlinear and additive, the UDRIM (s = 1) offers the best computational efficiency. Its cost scales linearly with the dimension, making it suitable for very high-dimensional problems. (ii) Screen for Interactions to Justify $s = 2$: the presence of significant interaction effects among input variables is the primary justification for employing the BDRIM ($s = 2$). The indicator function $Q_G(\Theta_{i_1},\Theta_{i_2})$ provides a quantitative tool for this screening. A pre-processing step that computes $Q_G(\Theta_{i_1},\Theta_{i_2})$ for a sample of variable pairs can identify if strong interactions are prevalent. If so, the BDRIM is necessary to capture the system's behavior accurately. This is the foundational idea behind adaptive methods like the Adaptive BDRIM [94] and the Hybrid DRM [89].

Analogous to UDRIM and BDRIM, the qth order raw moment of Z derived from multiplicative univariate and bivariate DRMs (M-UDRM and M-BDRM) is expressed as [86, 87, 95, 96]:

$$M_{Z,q} \approx \begin{cases} [G(\boldsymbol{\theta}_c)]^{1-N_{\mathrm{dim}}}\prod\limits_{i=1}^{N_{\mathrm{dim}}}\mathbb{E}\left[\left(G\left(\Theta_i,\underline{\boldsymbol{\theta}}_{i,c}\right)\right)^q\right], & s=1; \\ [G(\boldsymbol{\theta}_c)]^{\frac{q(N_{\mathrm{dim}}-1)(N_{\mathrm{dim}}-2)}{2}}\dfrac{\prod\limits_{1\leqslant i_1<i_2\leqslant N_{\mathrm{dim}}}\mathbb{E}\left[G\left(\Theta_{i_1},\Theta_{i_2},\underline{\boldsymbol{\theta}}_{i_1i_2,c}\right)^q\right]}{\prod\limits_{i=1}^{N_{\mathrm{dim}}}\mathbb{E}\left[G\left(\Theta_i,\underline{\boldsymbol{\theta}}_{i,c}\right)\right]^{q(N_{\mathrm{dim}}-2)}}, & s=2 \end{cases} \tag{34}$$

in which $\mathbb{E}\left[G\left(\Theta_i,\underline{\boldsymbol{\theta}}_{i,c}\right)^q\right]$ and $\mathbb{E}\left[\left(G\left(\Theta_i,\Theta_j,\underline{\boldsymbol{\theta}}_{ij,c}\right)\right)^q\right]$ in equation (34) are computed via GQR. Equation (34) defines the M-UDRIM for $s = 1$, and the multiplicative M-BDRIM for $s = 2$. Notably, equation (34) was derived by applying the multiplicative dimension-reduction model to the moment function $(G(\boldsymbol{\Theta}))^q$ or $(G(\boldsymbol{\Theta})-\mu_Z)^q$, specifically for $s = 2$. However, since the component functions $G\left(\Theta_{i_1},\Theta_{i_2},\underline{\boldsymbol{\theta}}_{i_1i_2,c}\right), 1\leqslant i_1 < i_2 \leqslant N_{\mathrm{dim}}$ and $G\left(\Theta_i,\underline{\boldsymbol{\theta}}_{i,c}\right), i = 1,2,\ldots,N_{\mathrm{dim}}$ in equation (34) are not necessarily mutually independent, the expectation of their product cannot be directly expanded [36]:

$$\begin{aligned} &\mathbb{E}\left[\frac{\prod\limits_{1\leqslant i_1<i_2\leqslant N_{\mathrm{dim}}} G\left(\Theta_{i_1},\Theta_{i_2},\underline{\boldsymbol{\theta}}_{i_1i_2,c}\right)^q}{\left[\prod\limits_{i=1}^{N_{\mathrm{dim}}} G\left(\Theta_i,\underline{\boldsymbol{\theta}}_{i,c}\right)\right]^{q(N_{\mathrm{dim}}-2)}}\right] \\ &\neq \frac{\prod\limits_{1\leqslant i_1<i_2\leqslant N_{\mathrm{dim}}}\mathbb{E}\left[G\left(\Theta_{i_1},\Theta_{i_2},\underline{\boldsymbol{\theta}}_{i_1i_2,c}\right)^q\right]}{\prod\limits_{i=1}^{N_{\mathrm{dim}}}\mathbb{E}\left[G\left(\Theta_i,\underline{\boldsymbol{\theta}}_{i,c}\right)\right]^{q(N_{\mathrm{dim}}-2)}}. \end{aligned} \tag{35}$$

To resolve this limitation, the idea of applying the multiplicative dimension-reduction model directly to the *original response function* $Z = G(\Theta)$ was proposed by Wang *et al* [36]. This approach yields the first q-order raw moments of Z as [36]

$$\begin{aligned} M_{Z,q} = &\sum_{l_1=1}^{m_{\mathrm{GH}}}\sum_{l_2=1}^{m_{\mathrm{GH}}}\cdots\sum_{l_{N_{\mathrm{dim}}}=1}^{m_{\mathrm{GH}}}\prod_{i=1}^{N_{\mathrm{dim}}} w_{i,l_i} \\ &\cdot\left[G\left(u_{1,l_1},u_{2,l_2},\ldots,u_{N_{\mathrm{dim}},l_{N_{\mathrm{dim}}}}\right)\right]^q \end{aligned} \tag{36}$$

$$
\begin{aligned}
&G\left(u_{1,l_1},u_{2,l_2},\ldots,u_{N_{\mathrm{dim}},l_{N_{\mathrm{dim}}}}\right)\\
&\approx \frac{\prod\limits_{\substack{k_1=s,s-2,\\ s-4,\ldots}}\left\{\left[\prod\limits_{\substack{1\leqslant i_1<i_2<\cdots\\ <i_{k_1}\leqslant N_{\mathrm{dim}}}} G\left(u_{i_1,l_1},u_{i_2,l_2},\ldots,u_{s_1-k_1,l_{s_1-k_1}},\underline{\boldsymbol{\theta}}_{i_1i_2\cdots i_{k_1},c}\right)\right]^{\binom{N_{\mathrm{dim}}-k_1-1}{s_1-k}}\right\}}{\prod\limits_{\substack{k_2=s-1,s-3,\\ s-5,\ldots}}\left\{\left[\prod\limits_{\substack{1\leqslant j_1<j_2<\cdots\\ <j_{k_2}\leqslant N_{\mathrm{dim}}}} G\left(u_{j_1,l_1},u_{j_2,l_2},\ldots,u_{s_2-k_2,l_{s_2-k_2}},\underline{\boldsymbol{\theta}}_{j_1j_2\cdots j_{k_2},c}\right)\right]^{\binom{N_{\mathrm{dim}}-k_2-1}{s_2-k}}\right\}}.
\end{aligned}
\tag{37}
$$

Particularly at truncation orders $s=2$, 3, equation (37) reduces to the following simplified forms:

$$
\begin{aligned}
&G\left(u_{1,l_1},u_{2,l_2},\ldots,u_{N_{\mathrm{dim}},l_{N_{\mathrm{dim}}}}\right)\\
&\approx \begin{cases}
\dfrac{\left[\prod\limits_{\substack{1\leqslant i_1<\\ i_2\leqslant N_{\mathrm{dim}}}} G\left(u_{i_1,l_{i_1}},u_{i_2,l_{i_2}},\underline{\boldsymbol{\theta}}_{i_1i_2,c}\right)\right][G(\boldsymbol{\theta}_c)]^{\frac{(N_{\mathrm{dim}}-1)(N_{\mathrm{dim}}-2)}{2}}}{\left[\prod\limits_{j=1}^{N} G\left(u_{j,l_j},\underline{\boldsymbol{\theta}}_{j,c}\right)\right]^{N_{\mathrm{dim}}-2}}, & s=2;\\
\dfrac{\left[\prod\limits_{\substack{1\leqslant i_1<i_2\\ <i_3\leqslant N_{\mathrm{dim}}}} G\left(u_{i_1,l_{i_1}},u_{i_2,l_{i_2}},u_{i_3,l_{i_3}},\underline{\boldsymbol{\theta}}_{i_1i_2i_3,c}\right)\right]\left[\prod\limits_{i=1}^{n} G\left(u_{i,l_i},\underline{\boldsymbol{\theta}}_{i,c}\right)\right]^{\binom{N_{\mathrm{dim}}-2}{2}}}{\left[\prod\limits_{\substack{1\leqslant j_1<\\ j_2\leqslant N_{\mathrm{dim}}}} G\left(u_{j_1,l_{j_1}},u_{j_2,l_{j_2}},\underline{\boldsymbol{\theta}}_{j_1j_2,c}\right)\right]^{\binom{N_{\mathrm{dim}}-3}{1}}[G(\boldsymbol{\theta}_c)]^{\binom{N_{\mathrm{dim}}-1}{3}}}, & s=3
\end{cases}.
\end{aligned}
\tag{38}
$$

The computational cost of moment estimation comprises two components: function evaluations and numerical integration operations. For complex engineering problems, function evaluation necessitates extensive structural re-analyses (e.g. large-scale finite element analysis and computational fluid dynamics simulations). Given that numerical integration costs are negligible compared to structural re-analysis expenses, computational efficiency is primarily gauged by function evaluation requirements. As evidenced by equations (36)–(38), while the dimensionality of numerical integration remains unchanged, function evaluation costs (and thus structural re-analyses) are substantially reduced, i.e. $\sum_{i=0}^{s} C_{N_{\mathrm{dim}}}^{i} m_{\mathrm{GH}}^{i}$ instead of $m_{\mathrm{GH}}^{N_{\mathrm{dim}}}$. For $s \ll N_{\mathrm{dim}}$ (e.g. $s=2$ or 3), this approach mitigates the curse of dimensionality in structural re-analysis. For the sake of clarity, equations (36)–(38) are noted as the GF-DRIM.

Furthermore, several enhanced techniques have been developed based on s-order truncated Va-DRMs [97–101],

such as the advanced decomposition schemes for two-dimensional integrals [97], the significant variable identification techniques [99, 100], and the increase in truncation order [101].

$$\begin{cases} \mu_Z = \sum_{i=1}^{p_t} \mu_{Gi} + (1-p_t)\, G(\boldsymbol{\theta}_{Sc}) \\ m_{Z,q} = \sum_{i=1}^{p_t} m_{Gi,q} + \sum\limits_{\substack{\sum_{i=1}^{p_t} \vartheta_i = q, q \geqslant 2 \\ \vartheta_i < q\,(i=1,\cdots,p_t)}} \binom{q}{l_1, l_2, \cdots, l_N} \prod_{1 \leqslant i \leqslant p_t} m_{Gi,\vartheta_i} \end{cases} \tag{39}$$

If $G_i(\boldsymbol{\Theta}_{Si})$ is a univariate function, its moments are computed as follows:

$$\begin{cases} \mu_{Gi} = \sum_{l_1=1}^{m_{\mathrm{GH}}} w_{1,l_1} G\left(u_{1,l_1}, \underline{\boldsymbol{\theta}}_{i,Sc}\right) \\ m_{Gi,q} = \sum_{a=1}^{m_{\mathrm{GH}}} w_{1,l_1} \left(G\left(u_{1,l_1}, \underline{\boldsymbol{\theta}}_{i,Sc}\right) - \mu_{Gi}\right)^q \end{cases} \tag{40}$$

where $\boldsymbol{\Theta}_i$ denotes a sub-vector of $\boldsymbol{\Theta}$ excluding Θ_i, and $\underline{\boldsymbol{\theta}}_{i,Sc}$ represents the reference points of $\boldsymbol{\Theta}_i$.

For $G_i(\boldsymbol{\Theta}_{Si})$ with multiple variables, the moments of $G_i(\boldsymbol{\Theta}_{Si})$ are evaluated by

$$\begin{aligned} \mu_{G_i} &= \mathbb{E}\left[G\left(\boldsymbol{\Theta}_{Si}, \underline{\boldsymbol{v}}_{i,Sc}\right)\right] \\ &= \sum_{l_1=1}^{m_{\mathrm{GH}}} \sum_{l_2=1}^{m_{\mathrm{GH}}} \cdots \sum_{l_{am}=1}^{m_{\mathrm{GH}}} w_{1,l_1} \ldots w_{d_{\mathrm{dim}},l_{d_{\mathrm{dim}}}} \\ &\quad \times G\left(u_{1,l_1}, u_{2,l_2}, \ldots, u_{d_{\mathrm{dim}},l_{d_{\mathrm{dim}}}}, \underline{\boldsymbol{v}}_{i,Sc}\right) \end{aligned} \tag{41}$$

$$\begin{aligned} M_{G_i,q} &= \mathbb{E}\left[G\left(\boldsymbol{\Theta}_{Si}, \underline{\boldsymbol{v}}_{i,Sc}\right) - \mu_{G_i}\right]^q \\ &\approx \sum_{l_1=1}^{m_{\mathrm{GH}}} \sum_{l_2=1}^{m_{\mathrm{GH}}} \cdots \sum_{l_{am}=1}^{m_{\mathrm{GH}}} w_{1,l_1} \ldots w_{d_{\mathrm{dim}},l_{d_{\mathrm{dim}}}} \\ &\quad \times \left[G\left(u_{1,l_1}, u_{2,l_2}, \ldots, u_{d_{\mathrm{dim}},l_{d_{\mathrm{dim}}}}, \underline{\boldsymbol{v}}_{i,Sc}\right) - \mu_{G_i}\right]^q \end{aligned} \tag{42}$$

where $\underline{\boldsymbol{v}}_{i,Sc}$ represents a sub-vector of $\boldsymbol{\theta}_{Sc}$ excluding corresponding coordinates of $\boldsymbol{\theta}_{Si}$. As equations (39)–(42) derive from the Ve-DRM, this computational framework is designated the VDRIM. In parallel, the M-VDRIM has been developed for fractional moments estimation [37]. Due to its reliance on nonlinear transformations, M-VDRIM is currently limited to fractional moments-based structural reliability analysis. Its extension to general moments estimation requires further investigation.

4.2. Ve-DRMs-based DRIMs

Based on the summation-form Ve-DRM, the moments of Z can be calculated as follows [88]:

4.3. H-DRM-based DRIMs

Based on the theoretical framework of the H-DRM, the first q-order raw moments $M_{Z,q}$ of system response Z are expressed as [89]

$$\begin{aligned} M_{Z,q} &= \sum_{i=1}^{p_v} \mathbb{E}\left[\left(G_i^{\mathrm{vec}} + \frac{G_{\mathrm{con}}}{p_t}\right)^q\right] + \sum_{i=1}^{p_t-p_v} \mathbb{E}\left[\left(G_i^{\mathrm{var}} + \frac{G_{\mathrm{con}}}{p_t}\right)^q\right] \\ &\quad + \sum_{\substack{\sum_{i=1}^{p_t} \vartheta_i = q, q \geqslant 2, \\ \vartheta_i < q\,(i=1,2,\cdots,p_t)}} \binom{q}{\vartheta_1, \vartheta_2, \cdots, \vartheta_{p_t}} \prod_{1 \leqslant i \leqslant p_v} \\ &\quad \times \mathbb{E}\left[\left(G_i^{\mathrm{vec}} + \frac{G_{\mathrm{con}}}{p_t}\right)^{\vartheta_i}\right] \prod_{1 \leqslant i \leqslant p_t - p_v} \mathbb{E}\left[\left(G_i^{\mathrm{var}} + \frac{G_{\mathrm{con}}}{p_t}\right)^{\vartheta_i}\right] \end{aligned} \tag{43}$$

Solving equation (43) requires evaluating integrals of $G_i^{\mathrm{vec}} + G_{\mathrm{con}}/p_t$ and $G_i^{\mathrm{var}} + G_{\mathrm{con}}/p_t$. Specifically, the q-order moments of $G_i^{\mathrm{vec}} + G_{\mathrm{con}}/p_t$ are determined through low-dimensional GQR:

$$\begin{aligned} &\mathbb{E}\left[\left(G_i^{\mathrm{vec}} + \frac{G_{\mathrm{con}}}{p_t}\right)^q\right] \\ &= \begin{cases} \sum_{l_1=1}^{m_{\mathrm{GH}}} w_{1,l_1} \left(G\left(u_{1,l_1}, \underline{\boldsymbol{\theta}}_{i_1,c}, \underline{\boldsymbol{v}}_{i,Sc}\right) + \frac{G_{\mathrm{con}}}{p_t}\right)^q, d_{\mathrm{dim}} = 1 \\ \sum_{l_1=1}^{m_{\mathrm{GH}}} \sum_{l_2=1}^{m_{\mathrm{GH}}} w_{1,l_1} w_{2,l_2} \left(G\left(u_{1,l_1}, u_{2,l_2}, \underline{\boldsymbol{\theta}}_{i_1 i_2,c}, \underline{\boldsymbol{v}}_{i,Sc}\right) + \frac{G_{\mathrm{con}}}{p_t}\right)^q, d_{\mathrm{dim}} = 2 \end{cases} \end{aligned} \tag{44}$$

For moments estimation of $G_i^{\mathrm{var}} + G_{\mathrm{con}}/p_t$, [89] directly apply dimension-reduction models to the *component functions* $G_i^{\mathrm{var}} + G_{\mathrm{con}}/p_t$ rather than the *moment functions*

$(G_i^{\text{var}} + G_{\text{con}}/p_t)^q$ to reduce the error caused by omitted interaction terms. Specifically,

$$\mathbb{E}\left[\left(G_i^{\text{var}} + \frac{G_{\text{con}}}{p_t}\right)^q\right] = \sum_{l_1=1}^{m_{\text{GH}}}\sum_{l_2=1}^{m_{\text{GH}}}\cdots\sum_{l_{d_{\text{dim}}}=1}^{m_{\text{GH}}}\prod_{j=1}^{d_{\text{dim}}} w_{j,l_j} \times\left[G_i\left(u_{1,l_1},u_{2,l_2},\ldots,u_{d_{\text{dim}},l_{d_{\text{dim}}}},\underline{\boldsymbol{v}}_{i,Sc}\right)+\frac{G_{\text{con}}}{p_t}\right]^q \tag{45}$$

in which $G_i(u_{1,l_1},u_{2,l_2},\ldots,u_{d_{\text{dim}},l_{d_{\text{dim}}}},\underline{\boldsymbol{v}}_{i,Sc})$ is characterized as the sum form of a series of low-dimensional component functions by equation (22) with $s=3$, i.e.

$$\begin{aligned} &G_i\left(u_{1,l_1},u_{2,l_2},\ldots,u_{d_{\text{dim}},l_{d_{\text{dim}}}},\underline{\boldsymbol{v}}_{i,Sc}\right)\\ &\approx\sum_{i_1<i_2<i_3} G_i\left(\Theta_{i_1},\Theta_{i_2},\Theta_{i_3},\underline{\boldsymbol{\theta}}_{i_1i_2i_3,c},\underline{\boldsymbol{v}}_{i,Sc}\right)-(N-3)\\ &\times\sum_{i_1<j_1} G_i\left(\Theta_{i_1},\Theta_{j_1},\boldsymbol{\theta}_{i_1j_1,c},\underline{\boldsymbol{v}}_{i,Sc}\right)+\frac{(N-2)(N-3)}{2}\\ &\times\sum_{q=1}^{n} G_i\left(\Theta_q,\boldsymbol{\theta}_{q,c},\underline{\boldsymbol{v}}_{i,Sc}\right)-\frac{(N-1)(N-2)(N-3)}{6}G(\boldsymbol{\theta}_c) \end{aligned} \tag{46}$$

in which $G_i(\Theta_{i_1},\Theta_{i_2},\Theta_{i_3},\underline{\boldsymbol{u}}_{i_1i_2i_3},\underline{\boldsymbol{v}}_{i,Sc})$ and $G_i(\Theta_{i_1},\Theta_{j_1},\underline{\boldsymbol{u}}_{i_1j_1},\underline{\boldsymbol{v}}_{i,Sc})$ are represented separately as

$$\begin{aligned} &G_i\left(\Theta_{i_1},\Theta_{i_2},\Theta_{i_3},\underline{\boldsymbol{\theta}}_{i_1i_2i_3},\underline{\boldsymbol{v}}_{i,Sc}\right)\\ &=Q_G\left(\Theta_{i_1},\Theta_{i_2},\Theta_{i_3}\right)G\left(\Theta_{i_1},\Theta_{i_2},\Theta_{i_3},\underline{\boldsymbol{\theta}}_{i_1i_2i_3},\underline{\boldsymbol{v}}_{i,Sc}\right)\\ &\quad+\left(1-Q_G\left(\Theta_{i_1},\Theta_{i_2},\Theta_{i_3}\right)\right)\left\{\sum_{j<t\leqslant 3}Q_G\left(\Theta_{i_j},\Theta_{i_t}\right)\right.\\ &\quad\times G\left(\Theta_{i_j},\Theta_{i_t},\underline{\boldsymbol{\theta}}_{i_ji_t},\underline{\boldsymbol{v}}_{i,Sc}\right)\\ &\quad+\sum_{j=1}^{3}\left(1-\sum_{t\leqslant 3,k\neq j}Q_G\left(\Theta_{i_j},\Theta_{i_t}\right)\right)\left(G\left(\Theta_{i_j},\underline{\boldsymbol{\theta}}_{i_j},\underline{\boldsymbol{v}}_{i,Sc}\right)\right.\\ &\quad\left.+G\left(\Theta_{i_t},\boldsymbol{\theta}_{i_t},\underline{\boldsymbol{v}}_{i,Sc}\right)\right)-\sum_{j=1}^{3}G\left(\Theta_{i_j},\underline{\boldsymbol{\theta}}_{i_j},\underline{\boldsymbol{v}}_{i,Sc}\right)\\ &\quad\left.+\left(\sum_{j<t\leqslant 3}Q_G\left(\Theta_{i_j},\Theta_{i_t}\right)-2\right)G_0\right\} \end{aligned} \tag{47}$$

$$\begin{aligned} &G_i\left(\Theta_{i_1},\Theta_{j_1},\underline{\boldsymbol{\theta}}_{i_1j_1},\underline{\boldsymbol{v}}_{i,Sc}\right)\\ &=Q_G\left(\Theta_{i_1},\Theta_{j_1}\right)G\left(\Theta_{i_1},\Theta_{j_1},\underline{\boldsymbol{\theta}}_{i_1j_1},\underline{\boldsymbol{v}}_{i,Sc}\right)\\ &\quad+\left[1-Q_G\left(\Theta_{i_1},\Theta_{j_1}\right)\right]\left[G\left(\Theta_{i_1},\underline{\boldsymbol{\theta}}_{i_1},\underline{\boldsymbol{v}}_{i,Sc}\right)\right.\\ &\quad\left.+G\left(\Theta_{j_1},\underline{\boldsymbol{\theta}}_{j_1},\underline{\boldsymbol{v}}_{i,Sc}\right)-G_0\right]. \end{aligned} \tag{48}$$

In summary, equations (43)–(48) synergistically integrate the advantages of both variable-based and VDRIMs. This approach is therefore designated as either the HDRIM or RDRIM.

4.4. Comparative analysis for DRIMs

The preceding sections have detailed a wide array of DRIMs. This section provides a comparative analysis of the reviewed DRIMs, synthesizing their relative advantages, limitations, and recommended use-case (applicability domains) as well as some technical comparison (e.g. admissible distributions, handling of dependence, algebraic precision) to form a practical selection guide. The summary and technical comparison are provided in tables 2 and 3.

- **UDRIM** offers the highest computational efficiency, making it feasible for very high-dimensional problems. However, it ignores all interactions, leading to potentially large truncation errors for systems with strong nonlinear couplings. It is best suited for initial scoping or for problems where the performance function is known to be nearly additive.
- **BDRIM** provides a good balance, capturing pairwise interactions. It serves as a robust general-purpose method for problems with low-to-moderate interaction strength. The adaptive BDRIM further enhances this by using interaction screening to reduce cost without sacrificing accuracy for non-interacting variable pairs.
- **M-UDRIM/M-BDRIM** are inherently suited for such systems and are particularly powerful for positive-valued response functions and fractional moment estimation, which is crucial for reliability analysis using the MEM. However, their application is complicated if the response can take non-positive values, often requiring nonlinear transformations that can introduce additional approximation error.
- **GF-DRIM** represents a different approach by applying a multiplicative DRM directly to the original function evaluations over a full-grid quadrature scheme. Its main advantage is high accuracy for a given truncation order s (e.g. $s=2$ or 3) as it better preserves the structure of the original function. The limitation is that its computational cost, while drastically lower than a full tensor product, is still high when s takes a relatively large value. Moreover, this method also requires the response function to be positive.
- **VDRIM** excels in accuracy for problems with clustered interactions by identifying statistically independent sub-vectors. Its performance is highly dependent on the vector classification; it can be very efficient if sub-vectors are low-dimensional, but costly if high-dimensional sub-vectors emerge.
- **HDRIM/RDRIM** synergizes the above approaches. It is the most versatile for complex systems with a mixture of strong localized interactions (handled by vector decomposition) and a large number of weakly contributing variables (handled by a secondary variable-based decomposition). The trade-off is increased implementation complexity.

Table 2. Critical comparison of DRIMs for moment estimation.

Method	Key advantage	Primary limitation	Recommended use-case
UDRIM	Highest computational efficiency; simple implementation	Neglects all interactions; large truncation error for coupled systems	High-dimensional screening; systems with weak/univariate effects
BDRIM	Good efficiency-accuracy balance; captures pairwise interactions	Inaccurate for strong higher-order (>2) interactions	Systems with significant pairwise interactions; General-purpose use for systems with low-to-moderate interaction strength
M-UDRIM/ M-BDRIM	Natural fit for multiplicative systems & positive-valued responses	Not directly suitable for non-positive responses; more complex moment derivation	Systems with positive outputs and multiplicative interactions
GF-DRIM	High accuracy for given truncation order s; preserves original function structure well	Higher cost if $s > 2$; Not directly suitable for non-positive responses	Problems requiring high accuracy with $s = 2$ or 3 where additive models show significant error
VDRIM	High accuracy	Cost can be prohibitive if vector classification yields high-dimensional sub-vectors	Systems that naturally decompose into independent, low-dimensional subsystems
HDRIM	Optimal balance for complex systems; versatile and robust	Highest implementation complexity	Systems with mixed interaction strengths (both strong localized and weak global effects)

Table 3. Technical comparison matrix of DRIMs.

Method	Admissible distributions	Handling of dependence	Algebraic precision
UDRIM	Any	Yes	Governed by 1D integration rule
BDRIM	Any	Yes	Governed by 2D integration rule
M-UDRIM/M-BDRIM	Positive-valued response	Yes	Governed by 1D/2D integration rule
GF-DRIM	Any	Yes	Governed by integration rule and truncation order
VDRIM	Any	Yes	Governed by integration rule for sub- vectors
HDRIM	Any	Yes	Governed by integration rule for sub-vectors

Notes on the table:
(i) Admissible distributions & handling of dependence: All DRIMs can handle non-Gaussian and dependent input variables through an initial iso-probabilistic transformation (e.g. Nataf or Rosenblatt transformation) to a space of independent standard Gaussian variables. The subsequent DRIM is then applied in this transformed space.
(ii) Algebraic precision: This refers to the highest polynomial order that the numerical integration scheme used for the component functions can integrate exactly. For example, if a 5-point GQR (9th order precision) is used for UDRIM's 1D integrals, the method can accurately capture moments influenced by up to 9th-order univariate terms.

5. Integration of dimension-reduction integration methods with advanced numerical integration algorithms

To enhance the computational efficiency of the DRIMs, advanced numerical integration algorithms have been incorporated to partially or fully replace GQR in DRIMs [53, 61–63, 102–105]. This section reviews three principal integration techniques synergistically integrated with DRIMs for moments estimation: the HUT method, CUT methods and SGI methods. A fundamental distinction between the advanced numerical integration algorithms discussed in this section (HUT, CUT, SGI) and the traditional tensor-product GQR lies in their approach to multidimensional integration. While the full tensor-product GQR constructs points by a combinatorial outer product of 1D quadrature rules, leading to an exponential growth of points $(m_{\mathrm{GH}})^{N_{\mathrm{dim}}}$, HUT, CUT, and SGI methods generate specialized, sparse point sets. These sets are strategically designed to achieve a high algebraic degree of precision for multidimensional integrals under specific probability measures (e.g. the standard Gaussian measure) using a significantly smaller number of points. The following subsections review these methods and their integration with DRIMs.

5.1. DRIM-HUT methods

The HUT method [106], developed from the foundational UT method [107, 108], was initially applied in nonlinear filtering. It has been progressively extended to high-order moments estimation and reliability analysis [59, 109, 110]. Recent research has integrated HUT with DRIMs [103, 104], yielding computational frameworks summarized below.

Within the BDRIM framework, the raw moments of Z are computed as:

$$M_{Z,q} \approx \sum_{i<j} \mathbb{E}\left[\left(G\left(\Theta_i, \Theta_j, \underline{\boldsymbol{\theta}}_{ij,c}\right)\right)^q\right] - (N_{\mathrm{dim}} - 2) \sum_{k=1}^{N_{\mathrm{dim}}} \times \mathbb{E}\left[\left(G\left(\Theta_k, \underline{\boldsymbol{\theta}}_{k,c}\right)\right)^q\right] + \frac{(N_{\mathrm{dim}} - 1)(N_{\mathrm{dim}} - 2)}{2} G^q\left(\boldsymbol{\theta}_c\right) \tag{49}$$

in which the one-dimensional integrals $\mathbb{E}\left[\left(G\left(\Theta_k, \underline{\boldsymbol{\theta}}_{k,c}\right)\right)^q\right]$ are evaluated via five-point GQR, while the two-dimensional integrals $\mathbb{E}\left[\left(G\left(\Theta_i, \Theta_j, \underline{\boldsymbol{\theta}}_{ij,c}\right)\right)^q\right]$ are computed using the HUT method. Specifically, the HUT method employs three distinct categories of integration points with associated weights, defined as follows [106]:

(1) Category I:

$$\boldsymbol{u}_0^h = \mathbf{0}, \quad w_0^h = \frac{-2{n_s}^2 + (4-2n_s)\,\alpha^2 + (4\alpha+4)\,n_s}{(n_s+\alpha)^2\,(4-n_s)} \tag{50}$$

where n_s represents the dimension of numerical integration. When HUT method is applied to equation (49), n_s is taken as 2.

(2) Category II:

$$\begin{cases} \boldsymbol{u}_{j_1}^h = \sqrt{\frac{(4-n_s)(n_s+\alpha)}{(\alpha+2-n_s)}}\mathbf{e}_{j_1} \\ \boldsymbol{u}_{j_1+n_s}^h = -\sqrt{\frac{(4-n_s)(n_s+\alpha)}{(\alpha+2-n_s)}}\mathbf{e}_{j_1}, \\ w_1^h = \frac{(\alpha+2-n_s)^2}{2(n_s+\alpha)^2(4-n_s)} \end{cases} \quad \begin{array}{l} j_1 = 1, \\ 2,\ldots,n_s \end{array} \tag{51}$$

in which $\mathbf{e}_{j_1} = [0,\ldots,0,1,0,\ldots,0]^{\mathrm{T}}$, i.e. the j_1th element of $\mathbf{e}_{j1}$ is 1.

(3) Category III:

$$\begin{cases} \boldsymbol{u}_{j_2}^h = +\sqrt{(n_s+\alpha)}\mathbf{s}_{j_2}^+ \\ \boldsymbol{u}_{j_2+0.5n_s(n_s-1)}^h = -\sqrt{(n_s+\alpha)}\mathbf{s}_{j_2}^+ \\ \boldsymbol{u}_{j_2+n_s(n_s-1)}^h = +\sqrt{(n_s+\alpha)}\mathbf{s}_{j_2}^-, \\ \boldsymbol{u}_{j_2+1.5n_s(n_s-1)}^h = -\sqrt{(n_s+\alpha)}\mathbf{s}_{j_2}^- \\ w_2^h = \frac{1}{(n_s+\alpha)^2} \end{cases} \quad \begin{array}{l} j_2 = 1,2,\ldots, \\ 0.5n_s\,(n_s-1) \end{array} \tag{52}$$

where $\left\{\mathbf{s}_{j_2}^+\right\} := \{\sqrt{1/2}(\mathbf{e}_k + \mathbf{e}_l) : k < l, k, l = 1,2,\ldots,n_s\}$, $\{\mathbf{s}_{j_2}^-\} := \{\sqrt{1/2}(\mathbf{e}_k - \mathbf{e}_l) : k < l, k, l = 1,2,\ldots,n_s\}$.

Notably, the parameter α in the HUT method significantly affects the accuracy of the moments estimation, which is recommended to set $\alpha = 7.2$ [103]. And the integration points of 2D space for the HUT method ($\alpha = 7.2$) are also displayed in figure 2. As illustrated in figure 2, although the HUT method and the 3-point GQR share identical computational cost and fifth-order algebraic accuracy, the integration points of the HUT method are situated at considerably greater distances from the origin compared to those of the 3-point GQR. This configuration may enable the HUT method to more effectively capture probabilistic tail characteristics of the integrand. Consequently, the numerical evaluation of two-dimensional integrals involving arbitrary functions is enhanced in accuracy, particularly for responses sensitive to distribution tails.

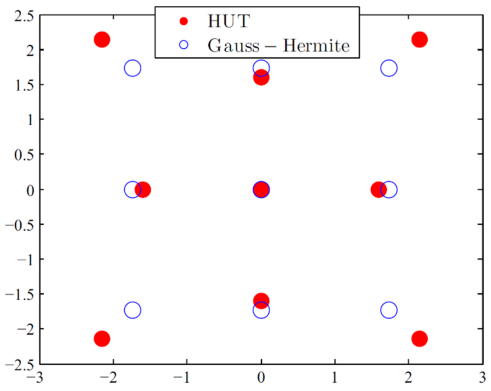


Figure 2. The integration points of 2D space for the HUT method ($\alpha = 7.2$) [103].

5.2. DRIM-CUT methods

The traditional CUT methods, also evolved from the UT method, comprise three variants: CUT4, CUT6 and CUT8, originally proposed by Adurthi *et al* [60]. Compared to UT and its derivatives, CUT methods achieve higher algebraic precision, with CUT4, CUT6 and CUT8 attaining fifth-, seventh- and ninth-order algebraic accuracy respectively. The dimensional constraints of traditional CUT methods might appear to limit their utility for high-dimensional global problems (e.g. CUT6 and CUT8 exhibit limited applicability to medium- and high-dimensional integration problems, constrained to dimensions $\leqslant 9$ for CUT6 and $\leqslant 6$ for CUT8 [63]), where the dimensional limits of these rules stem from the theoretical and combinatorial challenges of their construction (The CUT rules are built by solving a system of moment-matching equations to determine the coordinates and weights of a near-minimal, symmetric point set. Beyond these limits, the system of equations may have no solution or require an impractically large number of points, defeating the purpose of an efficient rule). However, this limitation is effectively circumvented by the very framework of DRIMs in which they are embedded. In practical implementation, CUT is not applied to the full high-dimensional function $G(\boldsymbol{\Theta})$. Instead, it is applied to the *component functions* generated by the Ve-DRM or H-DRM decomposition. The vector classification process in these models actively partitions the input variables into sub-vectors $\boldsymbol{\Theta}_{Si}$. A key practical step is to ensure that the dimension d_{dim} of each of these sub-vectors is intentionally managed to be within the operational range of the desired CUT rule. If a sub-vector resulting from the primary decomposition still has a dimensionality exceeding the CUT limit, a secondary decomposition using an additive Va-DRM (e.g. BDRIM) can be applied specifically to that component. This recursive strategy—using Ve-DRM/H-DRM for the primary decomposition and Va-DRM for any remaining high-dimensional components—creates a hierarchical integration scheme. This ensures that all final numerical integrations are performed over low-dimensional spaces where high-order rules like CUT6 and CUT8 are both applicable and highly efficient. Therefore, through this multi-level dimension-reduction approach, the high accuracy of advanced CUT methods can be leveraged for stochastic systems of virtually any dimension.

Concretely, Wang *et al* [61–63] proposed the ECUT methods through synergistic integration of DRIMs and variable transformation technique. This innovation extends applicability to arbitrary-dimensional problems with diverse

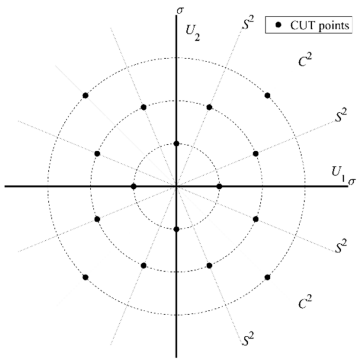


Figure 3. The axes and the reference points of 2D space for the CUT methods [63].

Table 4. The comparison of number of integration points for CUT methods and GQR.

Method	Number of points				
	$N_{\text{dim}}=2$	$N_{\text{dim}}=3$	$N_{\text{dim}}=4$	$N_{\text{dim}}=5$	$N_{\text{dim}}=6$
CUT4	9	15	25	43	77
3-point GQR	9	27	81	243	729
CUT6	13	27	49	83	137
4-point GQR	16	64	256	1024	4096
CUT8	21	59	161	355	745
5-point GQR	25	125	625	3125	15 625

variable distributions. By integrating the VDRIM into traditional CUT methods for moments estimation of $G(\boldsymbol{\Theta}_{Si})$ with multiple variables, the moments of $G(\boldsymbol{\Theta}_{Si})$ in equation (39) are derived as follows [63]:

$$\mu_{Gi}=\mathbb{E}\left[G\left(\boldsymbol{\Theta}_{Si},\underline{\boldsymbol{y}}_{i,Sc}\right)\right]=\sum_{i=0}^{m_{\text{CUT}}-1}w_i^c G\left(u_{1,i}^c,u_{2,i}^c,\ldots,u_{d_{\text{dim}},i}^c,\underline{\boldsymbol{y}}_{i,Sc}\right) \tag{53}$$

$$\begin{aligned} m_{G_i,q}&=\mathbb{E}\left[G\left(\boldsymbol{\Theta}_{Si},\underline{\boldsymbol{y}}_{i,Sc}\right)-\mu_{G_i}\right]^q \\ &=\sum_{i=0}^{m_{\text{CUT}}-1}w_i^c\left[G\left(u_{1,i}^c,u_{2,i}^c,\ldots,u_{d_{\text{dim}},i}^c,\underline{\boldsymbol{y}}_{i,Sc}\right)-\mu_{G_i}\right]^q \end{aligned} \tag{54}$$

where m_{CUT} denotes the number of abscissas for CUT methods, $\boldsymbol{u}_i^c=\{\boldsymbol{u}_{1,i}^c,u_{2,i}^c,\ldots,u_{d_{\text{dim}},i}^c\}$ and w_i^c represent the abscissas and weighs for CUT methods, respectively, which is computed as follows [63, 111]

$$\begin{cases} \boldsymbol{u}_0^c=\boldsymbol{0},w_0^c=w_0; \\ \boldsymbol{u}_i^c=r_1\sigma_i,w_i^c=w_1,\quad \text{for } 1\leqslant i\leqslant 2n_s; \\ \boldsymbol{u}_{i+2n_s}^c=r_2c_i^n,w_{i+2n_s}^c=w_2,\text{for } 1\leqslant i\leqslant 2^{n_s}; \\ \boldsymbol{u}_{i+2n_s+2^{n_s}}^c=r_3c_i^2,w_{i+2n_s+2^{n_s}}^c=w_3,\text{for } 1\leqslant i\leqslant 2n_s{}^2-2n_s; \\ \boldsymbol{u}_{i+2^{n_s}+2n_s{}^2}^c=r_4c_i^{n_s},w_{i+2^{n_s}+2n_s{}^2}^c=w_4,\text{for } 1\leqslant i\leqslant 2^n n_s; \\ \boldsymbol{u}_{i+2^{n_s+1}+2n_s{}^2}^c=r_5c_i^{n_s},w_{i+2^{n_s+1}+2n_s{}^2}^c=w_5,\text{for } 1\leqslant i\leqslant n_1; \\ \boldsymbol{u}_{i+n_1+2^{n_s+1}+2n_s{}^2}^c=r_6s_i^{n_s}(h_s),w_{i+n_1+2^{n_s+1}+2n_s{}^2}^c=w_6,\text{for } 1\leqslant i\leqslant n_s2^{n_s}; \\ n_1=\dfrac{4n_s(n_s-1)(n_s-2)}{3}. \end{cases} \tag{55}$$

Herein, r_i and w_i are computed via equation (56) for the CUT4 method. For CUT6 and CUT8 methods, these parameters are respectively tabulated in appendix A (tables A1 and A2). The reference point sets σ_i, c_i^m and $s_i^{n_s}(h_s)$ are defined by equation (57), while figure 3 illustrates the coordinate axes and reference points in 2D space for the CUT methods. Besides, the comparison of number of integration points for CUT methods and GQR is listed in table 4. This comparative analysis reveals that for a given level of algebraic accuracy, the CUT methods exhibit a substantially reduced computational cost relative to the GQR. This efficiency advantage becomes particularly pronounced in high-dimensional problems, where

the number of function evaluations required by GQR grows exponentially, while that of the CUT methods increases at a markedly slower rate. Consequently, the CUT methods offer superior computational efficiency while maintaining equivalent numerical precision.

$$\begin{cases} w_0 = 1 - 2n_s w_1 - 2^{n_s} w_2 \\ r_1 = \sqrt{\dfrac{n_s+2}{2}}; \quad w_1 = \dfrac{4}{(n_s+2)^2} \\ r_2 = \sqrt{\dfrac{n_s+2}{n_s-2}}; \quad w_2 = \dfrac{(n_s-2)^2}{2^{n_s}(n_s+2)^2} \end{cases} \tag{56}$$

$$\begin{cases} \sigma_i \in \{(\pm \mathbf{e}_k) \,|k \subset \mathbb{Z}\}, i = 1,2,\ldots,2n_s, \mathbb{Z} = \{1,2,\ldots,n_s\} \\ c_i^m \in \left\{ (\pm\mathbf{e}_1, \pm\mathbf{e}_2, \ldots, \pm\mathbf{e}_{n_s}) \middle| \mathbf{e}_j \in \{0,1\} \bigcap \sum_{j=1}^{n_s} \mathbf{e}_j = m \right\}, \\ \quad 2 \leqslant m \leqslant n_s, i = 1,2,\ldots,2^m C_{n_s}^m \\ s_i^{n_s}(h_s) \in \left\{ (\pm\mathbf{e}_1, \pm\mathbf{e}_2, \ldots, \pm\mathbf{e}_{n_s}) \middle| \mathbf{e}_j \in \{h_s,1\} \bigcap \sum_{j=1}^{n_s} \mathbf{e}_j = n_s - 1 + h_s \right\}, \\ \quad i = 1,2,\ldots,n_s 2^{n_s} \end{cases} \tag{57}$$

in which h_s represents a scaling parameter.

When the dimensions of $G(\boldsymbol{\Theta}_{Si})$ are still greater than the dimensional limits of CUT methods, the moments of $G(\boldsymbol{\Theta}_{Si})$ are calculated by [63]

$$\begin{aligned} \mu_{G_i} \approx & \sum_{\zeta<\varsigma} \mathbb{E}\left[Q_G(\Theta_{Si,\zeta}, \Theta_{Si,\varsigma}) G(\Theta_{Si,\zeta}, \Theta_{Si,\varsigma}, \underline{\boldsymbol{\theta}}_{\zeta\varsigma,ic}, \underline{\boldsymbol{v}}_{i,Sc}) \right. \\ & + (1 - Q_G(\Theta_{Si,\zeta}, \Theta_{Si,\varsigma})) \\ & \left. \times \begin{pmatrix} G(\Theta_{Si,\zeta}, \underline{\boldsymbol{\theta}}_{\zeta,ic}, \underline{\boldsymbol{v}}_{i,Sc}) \\ + G(\Theta_{Si,\varsigma}, \underline{\boldsymbol{\theta}}_{\varsigma,ic}, \underline{\boldsymbol{v}}_{i,Sc}) - G(\underline{\boldsymbol{\theta}}_{ic}, \underline{\boldsymbol{v}}_{i,Sc}) \end{pmatrix} \right] \\ & - (N-2) \sum_{t=1}^{d_{\dim}} \mathbb{E}\left[G(\Theta_{Si,t}, \underline{\boldsymbol{\theta}}_{t,ic}, \underline{\boldsymbol{v}}_{i,Sc}) \right] \\ & + \frac{(N-1)(N-2)}{2} G(\boldsymbol{\theta}_{Sc}) \end{aligned} \tag{58}$$

$$\begin{aligned} m_{G_i,q} \approx & \sum_{\zeta<\varsigma} \mathbb{E}\left[\left(Q_G(\Theta_{Si,\zeta}, \Theta_{Si,\varsigma}) G(\Theta_{Si,\zeta}, \Theta_{Si,\varsigma}, \underline{\boldsymbol{\theta}}_{\zeta\varsigma,ic}, \underline{\boldsymbol{v}}_{i,Sc}) \right. \right. \\ & + (1 - Q_G(\Theta_{Si,\zeta}, \Theta_{Si,\varsigma})) \\ & \times \begin{pmatrix} G(\Theta_{Si,\zeta}, \underline{\boldsymbol{\theta}}_{\zeta,ic}, \underline{\boldsymbol{v}}_{i,Sc}) \\ + G(\Theta_{Si,\varsigma}, \underline{\boldsymbol{\theta}}_{\varsigma,ic}, \underline{\boldsymbol{v}}_{i,Sc}) - G(\underline{\boldsymbol{\theta}}_{ic}, \underline{\boldsymbol{v}}_{i,Sc}) \end{pmatrix} \\ & \left. \left. - \mu_{G_i} \right)^q \right] - (N-2) \sum_{t=1}^{d_{\dim}} \mathbb{E}\left[\left(G(\Theta_{Si,t}, \underline{\boldsymbol{\theta}}_{t,ic}, \underline{\boldsymbol{v}}_{i,Sc}) \right)^q \right] \\ & + \frac{(N-1)(N-2)}{2} \left(G(\boldsymbol{\theta}_{Sc}) - \mu_{G_i} \right)^q \end{aligned} \tag{59}$$

in which $\underline{\boldsymbol{\theta}}_{t,ic}$ and $\underline{\boldsymbol{\theta}}_{\zeta\varsigma,ic}$ denote sub-vectors of $\boldsymbol{\theta}_{Si,c}$ excluding corresponding coordinates of $\Theta_{Si,t}$, $\Theta_{Si,\zeta}$ and $\Theta_{Si,\varsigma}$ respectively. For the two-dimensional integral in equations (58) and (59) when $Q_G(\Theta_{Si,\zeta}, \Theta_{Si,\varsigma}) = 1$, the abscissas $\boldsymbol{u}_i^c$ and weights w_i^c from two-dimensional CUT methods are employed. All one-dimensional integrals are evaluated using GQR.

5.3. DRIM-SGI methods

Traditional SGI methods leverage the Smolyak algorithm to construct specialized tensor rules that eliminate integration points with minimal accuracy contributions. The sparse grid point set is defined as [112–119]

$$\begin{aligned} \mathbf{N}(\boldsymbol{\Theta}) = & \bigcup_{\xi+1 \leqslant |a| \leqslant \xi+N_{\dim}} \mathbf{N}_1^{\xi}(\boldsymbol{\Theta}_1) \otimes \mathbf{N}_2^{\xi}(\boldsymbol{\Theta}_2) \\ & \otimes \ldots \mathbf{N}_i^{\xi}(\boldsymbol{\Theta}_i) \otimes \ldots \otimes \mathbf{N}_{N_{\dim}}^{\xi}(\boldsymbol{\Theta}_{N_{\dim}}) \end{aligned} \tag{60}$$

in which $\mathbf{N}_i^{\xi}(\boldsymbol{\Theta}_i)$ represents the nodal coordinates of the ith-dimension at level ξ, ξ represents a non-negative integer signifying the precision level; $\otimes$ denotes the tensor product operator; and $\boldsymbol{a} = (a_1, a_2, \ldots, a_{N_{\dim}})$ denotes a multi-index vector with $\|\boldsymbol{a}\|_1 = \sum_{i=1}^{N_{\dim}} a_i$.

Although traditional SGI methods enhance computational efficiency compared to full tensor-product integration, they still suffer from significantly growing computational costs with increasing dimensionality and precision requirements, as quantified in table 5. To mitigate this limitation, the point mapping strategy (PMS)-SGI method was proposed [53]. This approach partitions the sparse grid point set into mutually exclusive subsets while strategically eliminating non-essential reference points, as visualized in figure 4.

According to the HDMR-based PMS [53], the sparse grid point set decomposes into subsets with distinct effective dimensions:

Table 5. The number of sparse grid points for $\xi = 2$ and 3 [53].

$N_{\text{dim}}(\xi=2)$	n_{SGI}	$n_{\text{SGI},1}$	$n_{\text{SGI},2}$	$N_{\text{dim}}(\xi=3)$	n_{SGI}	$n_{\text{SGI},1}$	$n_{\text{SGI},2}$	$n_{\text{SGI},3}$
5	61	21	40	5	241	41	120	80
10	221	41	180	10	1581	81	540	960
15	481	61	420	15	5021	121	1260	3640
20	841	81	760	20	11 561	161	2280	9120
25	1301	101	1200	25	22 201	201	3600	18 400
30	1861	121	1740	30	37 941	241	5220	32 480

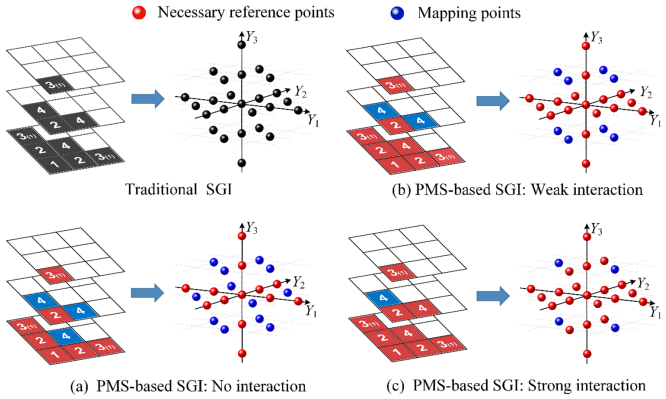


Figure 4. The integration points of traditional SGI and PMS-based SGI methods for ξ, $N_{\text{dim}} = 3$ [53].

$$\boldsymbol{a} \in T(\xi, N_{\text{dim}}) = \left\{1 \leqslant a_i \in N^+ \,(i = 1, \ldots, N_{\text{dim}}) : \xi + 1 < |a| \leqslant \xi + N_{\text{dim}}\right\} \tag{61}$$

$$T(\xi, N_{\text{dim}}) = \left\{ \begin{array}{l} T_1(\xi, N_{\text{dim}}) = \{\boldsymbol{a} = (1, \ldots, a_i, \ldots, 1) : a_i \geqslant 1, i = 1, \ldots, N_{\text{dim}}\} \\ T_2(\xi, N_{\text{dim}}) = \\ \{\boldsymbol{a} = (1, \ldots, a_{i_1}, \ldots, a_{i_2}, \ldots, 1) : a_{i_1} \geqslant 2, a_{i_2} \geqslant 2, 1 \leqslant i_1 < i_2 \leqslant N_{\text{dim}}\} \\ \vdots \\ T_\beta(\xi, N_{\text{dim}}) = \\ \left\{ \begin{array}{l} \text{if } \xi < N_{\text{dim}}, \boldsymbol{a} = (1, \ldots, a_1, \ldots, a_2, .., a_i, \ldots, 1) : a_i = 2, i = 1, \ldots, \xi \\ \text{if } \xi \geqslant N_{\text{dim}}, \boldsymbol{a} = (a_1, a_2, \ldots, a_{N_{\text{dim}}}) : a_i \geqslant 2, i = 1, \ldots, N_{\text{dim}} \end{array} \right\} \end{array} \right. \tag{62}$$

in which $\beta = \min\{\xi, N_{\text{dim}}\}$ denotes number of exclusive subsets.

Based on equation (62), the sparse grid points are represented as follows:

$$\begin{aligned} \underbrace{N(\Theta_1, \Theta_2, \ldots, \Theta_{N_{\text{dim}}})}_{a \in T(\xi, N_{\text{dim}})} = & \underbrace{\mathbf{R}_1(\Theta_i, \mathbf{0})}_{a \in T_1(\xi, N_{\text{dim}})} \cup \underbrace{\mathbf{R}_2(\Theta_{i_1}, \Theta_{i_2}, \mathbf{0})}_{a \in T_2(\xi, N_{\text{dim}})} \cup \\ & \cdots \cup \underbrace{\mathbf{R}_\xi\left(\Theta_{i_1}, \Theta_{i_2}, \ldots, \Theta_{i_{N_{\text{dim}}}}, \mathbf{0}\right)}_{a \in T_\xi(\xi, N_{\text{dim}})}. \end{aligned} \tag{63}$$

By means of equation (63), $M_{G,q}$ can be represented as a sum of multiple integrals over the sparse grid point sets with distinct effective dimensions [53]

$$\begin{aligned} M_{G,q} = & \sum_{a \in T_1(\xi, N_{\text{dim}})} M_{G_1,q}(\Theta_i) + \sum_{a \in T_2(\xi, N_{\text{dim}})} M_{G_2,q}(\Theta_{i_1}, \Theta_{i_2}) \\ & + \ldots + \sum_{a \in T_\xi(\xi, N_{\text{dim}})} M_{G_\xi,q}\left(\Theta_{i_1}, \Theta_{i_2}, \ldots, \Theta_{i_{N_{\text{dim}}}}\right) \end{aligned} \tag{64}$$

$$\begin{cases} M_{G_1,q}(\Theta_i) = \psi \cdot \sum_{i=1}^{m_i} w_i [G(u_i, \mathbf{0})]^q \\ M_{G_2,q}(\Theta_{i_1}, \Theta_{i_2}) = \psi \cdot \sum_{i_1=1}^{m_{i_1}} \sum_{i_2=1}^{m_{i_2}} w_{i_1} w_{i_2} [G(u_{i_1}, u_{i_2}, \mathbf{0})]^q \\ \cdots \\ M_{G_\xi,q}\left(\Theta_{i_1}, \Theta_{i_2}, \ldots, \Theta_{i_\xi}\right) = \psi \cdot \sum_{i_1=1}^{m_{i_1}} \sum_{i_2=1}^{m_{i_2}} \cdots \sum_{i_\xi=1}^{m_{i_q}} w_{i_1} w_{i_2} \ldots w_{i_\xi} \left[G\left(u_{i_1}, u_{i_2}, \ldots, u_{i_\xi}, \mathbf{0}\right)\right]^q \end{cases} \tag{65}$$

$$\begin{cases} G(u_{i_1}, u_{i_2}, \mathbf{0}) = Q_G(\Theta_{i_1}, \Theta_{i_2}) \underbrace{G(u_{i_1}, u_{i_2}, \mathbf{0})}_{\mathbf{R}_2(\Theta_{i_1}, \Theta_{i_2}, \mathbf{0})} + (1 - Q_G(\Theta_{i_1}, \Theta_{i_2})) \\ \qquad \cdot \underbrace{[G(u_{i_1}, \mathbf{0}) + G(u_{i_2}, \mathbf{0}) - G(\mathbf{0})]}_{\mathbf{R}_1(\Theta_i, \mathbf{0})} \\ G\left(u_{i_1}, u_{i_2}, \ldots, u_{i_\xi}, \mathbf{0}\right) = G_0 + \sum_{j \subset \left\{i_1, i_2, \ldots, i_l\right\}} G_j(u_j) + \sum_{\{i,j\} \subset \left\{i_1, i_2, \ldots, i_l\right\}} Q_G(\Theta_i, \Theta_j) \\ G_{ij}(u_i, u_j) + \ldots + Q_G\left(\Theta_{i_1}, \Theta_{i_2}, \ldots, \Theta_{i_\xi}\right) G_{i_1 i_2, \ldots, i_\xi}\left(u_{i_1}, u_{i_2}, \ldots, u_{i_\xi}, \mathbf{0}\right) \end{cases} \tag{66}$$

in which u_{i_l} and w_{i_l} are abscissas and weights obtained by the univariate GQR, respectively; ψ and m_i severally denote the additional weight factor and the number of nodes in the ith-dimension, namely

$$\begin{aligned} \psi &= (-1)^{\xi + N_{\dim} - |a|} \begin{pmatrix} N_{\dim} - 1 \\ \xi + N_{\dim} - |a| \end{pmatrix}, \\ m_i &= \begin{cases} \eta(a_i), \text{ if } a_i > 1 \\ 1, \text{ if } a_i = 1 \end{cases} \end{aligned} \tag{67}$$

where $\eta(a_i)$ represents a sequence function, e.g. $\eta(a_i) = 2a_i$–1.

6. Challenges and development trends in dimension-reduction integration methods

Notwithstanding significant advancements in DRIMs development over the past twenty years, the field persists as highly active. Considerable opportunities for future research exist, concomitant with challenges and future research directions requiring further investigation.

6.1. Advancing theoretical foundations

(i) **Adaptive dimension-reduction models:** Future research should focus on developing intelligent, data-driven frameworks that can autonomously determine the optimal form and complexity of the dimension-reduction model. This involves creating models that can adaptively select the appropriate truncation order s or even switch between additive and multiplicative formulations based on the characterized behavior of the response function. Such frameworks could leverage preliminary surrogate models or global sensitivity analysis to identify significant variables and interaction patterns, thereby tailoring the decomposition structure to the specific problem for enhanced accuracy and efficiency without prior user knowledge of the system's physics.

(ii) **Optimal integration strategies:** Formulating computationally efficient, high-accuracy point selection techniques with inherent numerical stability. Current implementations often rely on heuristics for selecting numerical integration schemes (e.g. the number of Gauss points) within DRIMs. A pressing challenge is the development of intelligent selection algorithms that optimally pair a specific DRIM with a numerical integration rule. These algorithms would balance computational cost and precision by considering factors such as the nonlinearity of the component functions and the target statistical moment order. Furthermore, research into novel, tailored quadrature rules that exploit the specific structure of the low-dimensional integrals generated by different DRIMs could yield significant efficiency gains over generic Gaussian quadrature.

(iii) **Nonlinear transformation techniques:** Conventional iso-probabilistic transformations (e.g. Nataf, Rosenblatt) are essential for handling non-Gaussian variables but can introduce severe nonlinearities into the performance function in the standard Gaussian space. This amplified nonlinearity can undermine the accuracy of the

subsequent low-order DRIM approximations. Further research is crucial to develop advanced transformation techniques or correction schemes that minimize this detrimental effect, thereby enhancing the robustness and accuracy of DRIMs for a wider range of input distributions.

(iv) **Interaction identification:** While methods for detecting variable interactions exist—such as global sensitivity analysis (e.g. Sobol indices [120, 121]) and the vector classification approach integral to Ve-DRMs—they often face significant computational bottlenecks in ultra-high-dimensional settings. Calculating high-order sensitivity indices for comprehensive screening remains prohibitively expensive. Future research is needed to develop computationally efficient, robust, and adaptive screening algorithms that can identify significant interactions with minimal function evaluations, potentially by leveraging machine learning or advanced sampling techniques.

(v) **Generalized adaptive frameworks:** Constructing algorithmic frameworks for intelligent DRIM selection across diverse engineering contexts. The ultimate goal is the creation of a meta-framework that automatically recommends or orchestrates the most suitable DRIM and its numerical settings for a given problem. This framework would intelligently analyze input dimensionality, correlation structure [92], estimated interaction strength (e.g. via global sensitivity indices [122–124]), and computational budget. By integrating modules for interaction screening, model selection, and integral evaluation, such a system would provide a robust, 'black-box' implementation of DRIMs, making these powerful methods accessible to non-specialists and ensuring near-optimal performance across a wide spectrum of applications in reliability and uncertainty quantification.

6.2. *Methodological expansion and applications*

(i) **Reliability analysis:** The primary application of DRIMs is to compute the statistical moments of a performance function. These moments are then used as input to advanced PDF reconstruction techniques, such as the moment-based density reconstruction [37, 63, 86] or polynomial chaos expansion [119–127], to accurately characterize the tail of the distribution and calculate the probability of failure without relying on costly MCS. The efficiency of DRIMs makes this approach feasible for complex, computationally intensive models.

(ii) **Design optimization under uncertainty:** DRIMs can be embedded within RBDO and RDO frameworks. In RBDO, DRIMs enable efficient estimation of probabilistic constraints during the optimization loop [128–131]. In RDO, they facilitate the calculation of the mean and variance of the system response, which are directly used as objectives or constraints [132, 133]. Their computational advantage is critical here, as optimization requires numerous repeated analyses.

(iii) **Risk and resilience assessment:** The role of moments extends to regional risk and system resilience evaluation. DRIMs can be used to construct fragility curves [3] which express the probability of exceeding a damage state given a hazard intensity by rapidly computing the moments of the structural response for a range of hazard levels. These fragility curves are fundamental components for probabilistic risk assessment and for quantifying the resilience of infrastructure systems against natural hazards like earthquakes and hurricanes [134–137].

6.3. *Integration and modularization of computing software*

Developing modular, embeddable software architectures for DRIMs is critical for bridging the gap between theoretical advancement and widespread engineering adoption. Future efforts should focus on:

(i) Creating standardized, application programming interfaces for DRIMs, allowing them to be easily integrated as solvers within larger stochastic finite element or computational fluid dynamics workflows, including commercial simulation platforms.

(ii) Developing open-source, community-driven toolboxes that consolidate various DRIMs and advanced numerical integration techniques, providing a unified environment for method comparison, validation, and hybridization.

(iii) Enhancing usability through the development of graphical user interfaces that guide users through the process of defining stochastic problems, selecting appropriate methods, and interpreting results, thereby democratizing access to these advanced techniques. This modularization will foster reproducibility, accelerate methodological development, and firmly embed DRIMs into the standard toolkit for computational engineering.

7. Conclusions

As a significant and effective means of estimating the moments of the stochastic system, the DRIMs have achieved systematic progress in the field of engineering uncertainty quantification and reliability analysis. The present work provides a comprehensive literature review on research related to the theoretical advances in dimension-reduction modeling, fundamental theory of DRIM frameworks, as well as integration with advanced numerical techniques. The significance of this review lies not in the presentation of novel numerical validations, which are abundantly available in the cited source material, but in its systematic organization of the fragmented

DRIMs landscape. By providing a clear taxonomy, elucidating the synergy between dimension-reduction models and numerical integration techniques, and outlining a roadmap for future research, this work aims to consolidate past advancements and accelerate future methodological developments and applications in engineering uncertainty quantification. The review also emphasizes the imperative for continued investigation in this field, especially for the deepening of theories in the aspects of dimension-reduction models and integration techniques, as well as the expansion of methods in reliability analysis, optimization design under uncertainty, and risk and resilience assessment. This constitutes a pivotal opportunity for methodological innovation and application of theoretical techniques by researchers.

Acknowledgments

This work is supported by the National Natural Science Foundation of China (Grant No. 52508584), the Natural Science Foundation of Chongqing (CSTB2024NSCQ-MSX1134) and the Research Grants Council of the Hong Kong Special Administrative Region, China (Project No T22–501/23-R). These supports are gratefully acknowledged.

Appendix. Parameters for conjugate unscented transform methods

Table A1. The values of r_i and w_i for CUT-6 method [63].

	Number of dimensions			
Variable	2	3	4	5
r_1	2.449 489 743	2.358 709 038	2.252 065 001	2.121 320 343
r_2	1.114 737 945	1.119 836 286	1.126 032 501	1.133 893 419
r_3	3.200 412 580	3.142 130 384	3.076 378 003	3.000 000 000
w_1	0.0277 777 78	0.029 035 130	0.030 660 163	0.032 921 811
w_2	0.130 287 665	0.063 384 461	0.030 660 163	0.014 703 361
w_3	0.000 465 301	0.000 519 547	0.000 589 837	0.000 685 871
w_0	0.365 877 024	0.312 478 971	0.249 999 999	0.172 839 506
	Number of dimensions			
Variable	6	7	8	9
r_1	1.948 835 279	2.551 200 355	2.449 489 743	2.343 906 881
r_2	1.144 596 894	0.964 263 098	0.999 999 999	1.023 262 187
r_3	2.906 800 606	2.325 576 698	2.449 489 743	2.534 286 566
w_1	0.036 507 256	0.012 694 063	0.013 888 888	0.015 076 408
w_2	0.006 948 717	0.004 859 446	0.002 343 750	0.001 134 272
w_3	0.000 828 855	0.000 395 089	0.000 231 481	0.000 157 273
w_0	0.067 463 712	0.089 648 847	0.074 074 074	0.042 189 853

Table A2. The values of r_i and w_i for CUT-8 method [63].

	Number of dimensions				
Variable	2	3	4	5	6
r_1	2.068 136 061	2.255 137 265	2.201 709 071	2.314 370 817	2.449 489 743
r_2	0.849 193 849	0.717 453 127	0.794 199 371	0.839 094 277	0.893 824 694
r_3	1.138 654 981	1.843 019 437	1.872 574 360	1.830 752 125	1.732 050 807
r_4	1.861 619 935	1.558 481 033	1.329 116 430	1.397 039 743	1.531 963 038
r_5	—	—	2	2	2
r_6	—	1.305 561 500	1.125 865 581	1.113 478 633	1.095 445 115
w_1	0.043 822 643	0.024 631 993	0.018 110 087	0.010 529 034	0.006 172 839
w_2	0.140 509 662	0.081 510 094	0.032 063 273	0.015 144 019	0.006 913 443
w_3	0.000 921 577	0.009 767 2355	0.006 614 353	0.005 282 899	0.004 115 226
w_4	0.012 409 539	0.005 772 489	0.003 489 906	0.001 067 129	0.000 218 327
w_5	—	—	0.000 651 042	0.000 651 042	0.000 651 0417
w_6	—	0.000 279 473	0.000 252 183	0.000 137 7602	0.000 078 4917
h_s	3	2.74	3	3	3

ORCID iD

Tao Wang 0000-0003-2718-7437

References

[1] Ang A H-S and Tang W H 2007 *Probability Concepts in Engineering* (Wiley)

[2] Sudret B and Der Kiureghian A 2000 *Stochastic Finite Element Methods and Reliability: a State-of-the-Art Report* (Department of Civil and Environmental Engineering, University of California)

[3] Wang C, Li Z, Wang T and Yu B 2023 Wind uplift fragility assessment method of 360° standing seam roof system and its application in wind damage estimation of UHV converter station *J. Struct. Eng.* **149** 04023031

[4] Ang A H S and De Leon D 2005 Modeling and analysis of uncertainties for risk-informed decisions in infrastructures engineering *Struct. Infrastruct. Eng.* **1** 19–31

[5] Chen B and Qian X 2025 Explainable data-driven analysis of uncertainty propagation in 3D concrete printing via adaptive polynomial chaos expansion *Autom. Constr.* **178** 106414

[6] Tang Z, Li Z and Wang T 2023 Probabilistic bearing capacity assessment for unequal-leg angle cross-bracings in transmission towers *J. Constructional Steel Res.* **200** 107672

[7] Rubinstein R Y and Kroese D P 2016 *Simulation and the Monte Carlo Method* (Wiley)

[8] Zhang H, Mahabadi R K, Rudin C, Guilleminot J and Brinson L C 2024 Uncertainty quantification of acoustic metamaterial bandgaps with stochastic material properties and geometric defects *Comput. Struct.* **305** 107511

[9] Joint Committee on Structural Safety (JCSS) 2001 Probabilistic model code-part 3-resistance models (JCSS-2001) (JCSS)

[10] Huyse L and Walters R W 2001 Random field solutions including boundary condition uncertainty for the steady-state generalized Burgers equation *Institute for Computer Applications in Science and Engineering* (NASA Langley Research Center)

[11] Tang Z, Li Z, Wang T, Lu D and Tan Y 2023 PDEM-based multi-component and global reliability evaluation framework for steel tubular transmission towers with semi-rigid connections *Eng. Struct.* **295** 116838

[12] Domeneghetti A, Vorogushyn S, Castellarin A, Merz B and Brath A 2013 Probabilistic flood hazard mapping: effects of uncertain boundary conditions *Hydrol. Earth Syst. Sci.* **17** 3127–40

[13] Tang Z, Li Z and Wang T 2022 GPR-based prediction and uncertainty quantification for bearing capacity of steel tubular members considering semi-rigid connections in transmission towers *Eng. Fail. Anal.* **142** 106854

[14] Pappenberger F, Matgen P, Beven K J, Henry J-B, Pfister L and Fraipont P 2006 Influence of uncertain boundary conditions and model structure on flood inundation predictions *Adv. Water Resour.* **29** 1430–49

[15] Ambrosini R D, Riera J D and Danesi R F 2002 Analysis of structures subjected to random wind loading by simulation in the frequency domain *Probab. Eng. Mech.* **17** 233–9

[16] Szafran J, Juszczyk K and Kamiński M 2020 Reliability assessment of steel lattice tower subjected to random wind load by the stochastic finite-element method *ASCE-ASME J. Risk Uncertain. Eng. Syst. A* **6** 04020003

[17] Wang B, Wang T, Li M, Li Z, Lu D and Tan Y 2025 Dynamic global reliability assessment of 500 kV tension suspension-braced transmission system *Proc. Chin. Soc. Electr. Eng.* **45** 2437–46

[18] Stewart M G, Ginger J D, Henderson D J and Ryan P C 2018 Fragility and climate impact assessment of contemporary housing roof sheeting failure due to extreme wind *Eng. Struct.* **171** 464–75

[19] Wang L, Wang T, Li Z, Lu D and Tan Y 2024 Stochastic seismic dynamic response analysis for coupled transmission tower-insulator-line systems considering soil-structure interaction *Soil Dyn. Earthq. Eng.* **181** 108662

[20] Deodatis G 1996 Non-stationary stochastic vector processes: seismic ground motion applications *Probab. Eng. Mech.* **11** 149–67

[21] Takahashi Y, Kiureghian A D and Ang A H S 2004 Life-cycle cost analysis based on a renewal model of earthquake occurrences *Earthq. Eng. Struct. Dyn.* **33** 859–80

[22] Suominen M, Kujala P, Romanoff J and Remes H 2017 Influence of load length on short-term ice load statistics in full-scale *Mar. Struct.* **52** 153–72

[23] Zvyagin P and Sazonov K 2014 Analysis and probabilistic modeling of the stationary ice loads stochastic process with lognormal distribution *Proc. ASME 2014 33rd Int. Conf. on Ocean, Offshore and Arctic Engineering* pp 8–13

[24] Wang T, Dong Y, Wang L, Lu D, Hu S, Tan Y and Li Z 2024 Global reliability assessment of coupled transmission

tower-insulator-line systems considering soil-structure interaction subjected to multi-hazard of wind and ice *J. Constructional Steel Res.* **223** 109004
[25] Wang T, Wang Z, Lu D, Tan Y and Li Z 2025 Galloping-induced global reliability assessment for ice-covered three-phase bundled conductors considering both mechanical and electrical functional failure modes *Reliab. Eng. Syst. Saf.* **262** 111240
[26] Anderson T W *et al* 1958 *An Introduction to Multivariate Statistical Analysis* (Wiley)
[27] Srivastava M S 2002 *Methods of Multivariate Statistics* (Wiley)
[28] Masuda-Jindo K, Van Hung V and Tam P D 2003 Thermodynamic quantities of metals investigated by an analytic statistical moment method *Phys. Rev. B* **67** 094301
[29] Zhao Y G and Lu Z H 2021 *Structural Reliability: Approaches from Perspectives of Statistical Moments* (Wiley)
[30] Pearson E S, Johnson N L and Burr I W 1979 Comparisons of the percentage points of distributions with the same first four moments, chosen from eight different systems of frequency curves *Commun. Stat. Simul. Comput.* **8** 191–229
[31] Broda S A and Paolella M S 2011 Saddlepoint approximations: a review and some new applications *Handbook of Computational Statistics: Concepts and Methods* (Springer) pp 953–83
[32] Zhao Y G and Lu Z H 2007 Fourth-moment standardization for structural reliability assessment *J. Struct. Eng.* **133** 916–24
[33] Krishnamoorthy K 2006 *Handbook of Statistical Distributions with Applications* (Chapman and Hall/CRC)
[34] Teitler S, Rajagopal A K and Ngai K L 1986 Maximum entropy and reliability distributions *IEEE Trans. Reliab.* **35** 391–5
[35] Wu F, Yao X, Gong J, Hu Y, Wang T and Zhao N 2024 A novel hybrid method for the stationary non-Gaussian wind pressures simulation based on maximum entropy method and moment-based translation function *Mech. Syst. Signal Process.* **210** 111167
[36] Wang T, Li Z, Fan W and Ang A H-S 2024 Structural system reliability assessment using generalized factorized dimensional reduction method and iterative maximum entropy method *Struct. Infrastruct. Eng.* **20** 607–18
[37] Wang L *et al* 2025 Structural reliability analysis based on fractional moments-based iterative maximum entropy method and multiplicative exact dimension reduction integration method *Reliab. Eng. Syst. Saf.* **264** 111344
[38] Gelman A 1995 Method of moments using Monte Carlo simulation *J. Comput. Graph. Stat.* **4** 36–54
[39] Yang X, Lu D, Jia M and Wang T 2024 Time-dependent seismic reliability analysis of rocking cold-formed steel frame based on improved HOMM *Thin-Walled Struct.* **200** 111878
[40] Liu C, Wang T, Tang Z and Li Z 2023 Time-varying wind-resistance global reliability analysis of in-service transmission tower using high-order moments-based improved maximum entropy method *Appl. Sci.* **13** 4245
[41] Rajabalinejad M 2010 Bayesian Monte Carlo method *Reliab. Eng. Syst. Saf.* **95** 1050–60
[42] Kennedy M 1998 Bayesian quadrature with non-normal approximating functions *Stat. Comput.* **8** 365–75
[43] O'Hagan A 1991 Bayes–hermite quadrature *J. Stat. Plan. Inference* **29** 245–60
[44] Rosenblueth E 1975 Point estimates for probability moments *Proc. Natl Acad. Sci.* **72** 3812–4
[45] Rosenblueth E 1981 Two-point estimates in probabilities *Appl. Math. Modelling* **5** 329–35
[46] Harr M E 1989 Probabilistic estimates for multivariate analyses *Appl. Math. Modelling* **13** 313–8
[47] Chang C H, Tung Y K and Yang J C 1995 Evaluation of probability point estimate methods *Appl. Math. Modelling* **19** 95–105
[48] Ko M and Papakonstantinou K G 2025 Quadratic point estimate method for probabilistic moments computation *Probab. Eng. Mech.* **79** 103705
[49] Zhou J and Nowak A S 1988 Integration formulas to evaluate functions of random variables *Struct. Saf.* **5** 267–84
[50] He J, Gao S and Gong J 2014 A sparse grid stochastic collocation method for structural reliability analysis *Struct. Saf.* **51** 29–34
[51] Xiong F, Greene S, Chen W, Xiong Y and Yang S 2010 A new sparse grid-based method for uncertainty propagation *Struct. Multidiscip. Optim.* **3** 335–49
[52] Guan X 2024 Sparse moment quadrature for uncertainty modeling and quantification *Reliab. Eng. Syst. Saf.* **241** 109665
[53] Wang T, Li J, Lu D, Dong Y, Tan Y and Li Z 2024 A point mapping strategy-based sparse grid integration method for statistical moments estimation and structural reliability analysis *Comput. Methods Appl. Mech. Eng.* **430** 117238
[54] Xu J and Lu Z H 2017 Evaluation of moments of performance functions based on efficient cubature formulation *J. Eng. Mech.* **143** 06017007
[55] Zhang D, Shen S, Jiang C, Han X and Li Q 2022 An advanced mixed-degree cubature formula for reliability analysis *Comput. Methods Appl. Mech. Eng.* **400** 115521
[56] Julier S J and Uhlmann J K 2004 Unscented filtering and nonlinear estimation *Proc. IEEE* **92** 401–22
[57] Maußner J and Freund H 2018 Optimization under uncertainty in chemical engineering: comparative evaluation of unscented transformation methods and cubature rules *Chem. Eng. Sci.* **183** 329–45
[58] Angrisani L, D'Apuzzo M and Moriello R S L 2005 The unscented transform: a powerful tool for measurement uncertainty evaluation *Proc. 2005 IEEE Int. Workshop on Advanced Methods for Uncertainty Estimation in Measurement* (IEEE) pp 27–32
[59] Xiao S and Lu Z 2018 Reliability analysis by combining higher-order unscented transformation and fourth-moment method *ASCE-ASME J. Risk Uncertain. Eng. Syst. A* **4** 04017034
[60] Adurthi N, Singla P and Singh T 2012 The conjugate unscented transform—an approach to evaluate multi-dimensional expectation integrals *2012 American Control Conf. (ACC)* (IEEE) pp 5556–61
[61] Wang T, Li Z and Fan W 2021 An uncertainty propagation analysis method for stochastic system based on extended conjugate unscented transform *Eng. Mech.* **38** 15–23
[62] Wang T, Li Z and Fan W 2022 Global reliability analysis of structures based on improved statistical moment point estimation method and maximum entropy principle *Eng. Mech.* **39** 193–200,211
[63] Wang T, Li Z, Fan W and Ang A H-S 2021 Structural reliability assessment based on enhanced conjugate unscented transformation and improved maximum entropy method *J. Struct. Eng.* **147** 04021213
[64] Blatman G and Sudret B 2010 An adaptive algorithm to build up sparse polynomial chaos expansions for stochastic finite element analysis *Probab. Eng. Mech.* **25** 183–97
[65] Shi Y, Lu Z, Chen S and Xu L 2018 A reliability analysis method based on analytical expressions of the first four moments of the surrogate model of the performance function *Mech. Syst. Signal Process.* **111** 47–67
[66] Rahman S and Xu H 2004 A univariate dimension-reduction method for multi-dimensional integration in stochastic mechanics *Probab. Eng. Mech.* **19** 393–408
[67] Xu H and Rahman S 2004 A generalized dimension-reduction method for multidimensional

integration in stochastic mechanics *Int. J. Numer. Methods Eng.* **61** 1992–2019
[68] Rahman S 2009 Stochastic sensitivity analysis by dimensional decomposition and score functions *Probab. Eng. Mech.* **24** 278–87
[69] Zhao Y G and Ono T 2001 Moment methods for structural reliability *Struct. Saf.* **23** 47–75
[70] Feng K, Lu Z Z, Li H, He P and Dai Y 2024 Dimensional reduction technique-based maximum entropy principal method for safety degree analysis under twofold random uncertainty *Probab. Eng. Mech.* **76** 103628
[71] Li H, Lu Z Z and Feng K 2024 A decoupling algorithm for efficient estimation of failure probability function based on statistical moment functions *J. Mech. Des.* **146** 101706
[72] Acevedo C H, Zhang X Y, Valdebenito M A and Faes M G R 2025 Reliability analysis combining method of moments with control variates *Probab. Eng. Mech.* **81** 103771
[73] Zhang Z, Jiang C, Han X and Ruan X X 2019 A high-precision probabilistic uncertainty propagation method for problems involving multimodal distributions *Mech. Syst. Signal Process.* **126** 21–41
[74] Zhao Y G and Ang A H S 2003 System reliability assessment by method of moments *J. Struct. Eng.* **129** 1341–9
[75] Wang T, Fan W, Ang A H S and Li Z 2023 Application of generalized equivalent extreme-value event in structural system reliability analysis *Struct. Infrastruct. Eng.* **19** 921–31
[76] Li P P, Lu Z H and Zhao Y G 2021 Bayesian updating of time-dependent structural reliability using the method of moment *ASCE-ASME J. Risk Uncertain. Eng. Syst. A* **7** 04021066
[77] Zhang X Y, Lu Z H, Wu S Y and Zhao Y-G 2021 An efficient method for time-variant reliability including finite element analysis *Reliab. Eng. Syst. Saf.* **210** 107534
[78] He W, Li G, Hao P and Zeng Y 2019 Maximum entropy method-based reliability analysis with correlated input variables via hybrid dimension-reduction method *J. Mech. Des.* **141** 101405
[79] Byeong H J and Lee B C 2008 Reliability-based design optimization using a moment method and a kriging metamodel *Eng. Optim.* **40** 421–38
[80] Wang T, Li Z, Fan W and Ang A H-S 2024 An adaptive hybrid dimension-reduction model and its application for statistical moments estimation of stochastic systems and reliability analysis of structures *Struct. Infrastruct. Eng.* **20** 653–65
[81] Rabitz H and Aliş Ö F 1999 General foundations of high-dimensional model representations *J. Math. Chem.* **25** 197–233
[82] Li G, Wang S and Rabitz H 2000 High dimensional model representations (HDMR): concepts and applications *Proc. Institute of Mathematics and Its Applications Workshop on Atmospheric Modeling* (Citeseer)
[83] Li G, Rosenthal C and Rabitz H 2001 High dimensional model representations *J. Phys. Chem. A* **105** 7765–77
[84] Tunga M A and Demiralp M 2005 A factorized high dimensional model representation on the nodes of a finite hyperprismatic regular grid *Appl. Math. Comput.* **164** 865–83
[85] Tunga M A and Demiralp M 2004 A factorized high dimensional model representation on the partitioned random discrete data *Appl. Numer. Anal. Comput. Math.* **1** 231–41
[86] Zhang X and Pandey M D 2013 Structural reliability analysis based on the concepts of entropy, fractional moment and dimensional reduction method *Struct. Saf.* **43** 28–40
[87] Zhang X, Pandey M D and Zhang Y 2014 Computationally efficient reliability analysis of mechanisms based on a multiplicative dimensional reduction method *J. Mech. Des.* **136** 061006
[88] Liu R, Fan W, Wang Y, Ang A H-S and Li Z 2019 Adaptive estimation for statistical moments of response based on the exact dimension reduction method in terms of vector *Mech. Syst. Signal Process.* **126** 609–25
[89] Wang T, Lu D G and Tan Y Q 2025 Refined dimension-reduction integration method for uncertainty propagation in stochastic systems: estimation of statistical moments *Reliab. Eng. Syst. Saf.* **256** 110753
[90] Rosenblatt M 1952 Remarks on a multivariate transformation *Ann. Math. Stat.* **23** 470–2
[91] Liu P L and Der Kiureghian A 1986 Multivariate distribution models with prescribed marginals and covariances *Probab. Eng. Mech.* **1** 105–12
[92] Song P, Wang T and Lu D G 2023 Structural global reliability assessment considering nonlinear correlation effects by enhanced high-order moment method *Acta Mech. Sin.* **39** 722356
[93] Huang X and Zhang Y 2013 Reliability–sensitivity analysis using dimension reduction methods and saddlepoint approximations *Int. J. Numer. Methods Eng.* **93** 857–86
[94] Fan W, Wei J, Ang A H S and Li Z 2016 Adaptive estimation of statistical moments of the responses of random systems *Probab. Eng. Mech.* **43** 50–67
[95] Balomenos G P, Genikomsou A S, Polak M A and Pandey M D 2015 Efficient method for probabilistic finite element analysis with application to reinforced concrete slabs *Eng. Struct.* **103** 85–101
[96] Balomenos G P and Pandey M D 2016 Finite element reliability and sensitivity analysis of structures using the multiplicative dimensional reduction method *Struct. Infrastruct. Eng.* **12** 1553–65
[97] Liu C, Fan W, Wang T, Wang Z and Li Z 2023 An efficient approach for statistical moments estimation of structural response based on a novel adaptive hybrid dimension-reduction method *Probab. Eng. Mech.* **73** 103484
[98] Youn B D, Xi Z and Wang P 2008 Eigenvector dimension reduction (EDR) method for sensitivity-free probability analysis *Struct. Multidiscip. Optim.* **37** 13–28
[99] Chen Z, Zhou P, Liu Y and Ji P 2019 A novel approach to uncertainty analysis using methods of hybrid dimension reduction and improved maximum entropy *Struct. Multidiscip. Optim.* **60** 1841–66
[100] Hu D Z, Lu Z H and Zhao Y G 2022 Estimation of statistical moments of performance functions using efficient importance measure *J. Asian Arch. Build. Eng.* **21** 1532–44
[101] Zhou Q, Li Z, Fan W, Ang A H-S and Liu R 2017 System reliability assessment of deteriorating structures subjected to time-invariant loads based on improved moment method *Struct. Saf.* **68** 54–64
[102] Ding C and Xu J 2021 An improved adaptive bivariate dimension-reduction method for efficient statistical moment and reliability evaluations *Mech. Syst. Signal Process.* **149** 107309
[103] Xu J and Dang C 2019 A new bivariate dimension reduction method for efficient structural reliability analysis *Mech. Syst. Signal Process.* **115** 281–300
[104] Xu J and Zhou L 2020 An adaptive trivariate dimension-reduction method for statistical moments assessment and reliability analysis *Appl. Math. Modelling* **82** 748–65
[105] Cai C H, Lu Z H, Xu J and Zhao Y-G 2019 Efficient algorithm for evaluation of statistical moments of performance functions *J. Eng. Mech.* **145** 06018007
[106] Jia B, Xin M and Cheng Y 2013 High-degree cubature Kalman filter *Automatica* **49** 510–8

[107] Julier S J 2003 The spherical simplex unscented transformation *Proc. 2003 American Control Conf.* (IEEE) vol 3 pp 2430–4
[108] Julier S J 2002 The scaled unscented transformation *Proc. 2002 American Control Conf. (IEEE Cat. No. CH37301)* (IEEE) vol 6 pp 4555–9
[109] Zhang Y G, Huang Y, Wu Z and Li N 2014 A high order unscented Kalman filtering method *Acta Autom. Sin.* **40** 838–48
[110] Zhang L W and Zhao Y G 2022 HUT-based method for structural reliability considering the non-normal and unknown distributions *Qual. Reliab. Eng. Int.* **38** 2303–23
[111] Li Z, Wang C and Wang T 2022 Reliability analysis of wind-uplifted resistance of standing seam roof system with anti-wind clips *J. Harbin Inst. Technol.* **54** 75–83
[112] Smolyak S 1963 *Quadrature and Interpolation Formulas for Tensor Products of Certain Classes of Functions* (Russian Academy of Sciences) pp 1042–5
[113] Holtz M 2010 *Sparse Grid Quadrature in High Dimensions with Applications in Finance and Insurance* (Springer)
[114] Haji-Ali A L, Harbrecht H, Peters M D and Siebenmorgen M 2018 Novel results for the anisotropic sparse grid quadrature *J. Complexity* **47** 62–85
[115] Holtz M 2010 Sparse grid quadrature *Sparse Grid Quadrature in High Dimensions with Applications in Finance and Insurance* (Springer) pp 51–76
[116] Singh A K, Radhakrishnan R, Bhaumik S and Date P 2018 Adaptive sparse-grid Gauss–Hermite filter *J. Comput. Appl. Math.* **342** 305–16
[117] Abay K A 2015 Evaluating simulation-based approaches and multivariate quadrature on sparse grids in estimating multivariate binary probit models *Econ. Lett.* **126** 51–56
[118] Wu J, Zhang D, Jiang C, Han X and Li Q 2021 On reliability analysis method through rotational sparse grid nodes *Mech. Syst. Signal Process.* **147** 107106
[119] Liu H B, Jiang C, Liu J and Mao J Z 2019 Uncertainty propagation analysis using sparse grid technique and saddlepoint approximation based on parameterized p-box representation *Struct. Multidiscip. Optim.* **59** 61–74
[120] Azzini I, Mara T A and Rosati R 2021 Comparison of two sets of Monte Carlo estimators of Sobol'indices *Environ. Modelling Softw.* **144** 105167
[121] Arnst M, Soize C and Bulthuis K 2021 Computation of sobol indices in global sensitivity analysis from small data sets by probabilistic learning on manifolds *Int. J. Uncertain. Quantification* **11** 1–23
[122] Yun W, Lu Z, He P, Jiang X and Dai Y 2020 Parameter global reliability sensitivity analysis with meta-models: a probability estimation-driven approach *Aerosp. Sci. Technol.* **106** 106040
[123] Li L, Papaioannou I and Straub D 2024 Efficient global sensitivity analysis method for dynamic models in high dimensions *Int. J. Numer. Methods Eng.* **125** e7494
[124] Li L, Papaioannou I and Straub D 2019 Global reliability sensitivity estimation based on failure samples *Struct. Saf.* **81** 101871
[125] Hu C and Youn B D 2011 Adaptive-sparse polynomial chaos expansion for reliability analysis and design of complex engineering systems *Struct. Multidiscip. Optim.* **43** 419–42
[126] Bhusal R and Subbarao K 2019 Uncertainty quantification using generalized polynomial chaos expansion for nonlinear dynamical systems with mixed state and parameter uncertainties *J. Comput. Nonlinear Dyn.* **14** 021011
[127] Zhang X, Pandey M D and Luo H 2021 Structural uncertainty analysis with the multiplicative dimensional reduction-based polynomial chaos expansion approach *Struct. Multidiscip. Optim.* **64** 2409–27
[128] Lee I, Choi K K and Gorsich D 2010 Sensitivity analyses of FORM-based and DRM-based performance measure approach (PMA) for reliability-based design optimization (RBDO) *Int. J. Numer. Methods Eng.* **82** 26–46
[129] Lee I, Choi K K, Du L and Gorsich D 2008 Dimension reduction method for reliability-based robust design optimization *Comput. Struct.* **86** 1550–62
[130] Wang Z, Li H, Chen Z, Li L and Hong H 2020 Sequential optimization and moment-based method for efficient probabilistic design *Struct. Multidiscip. Optim.* **62** 387–404
[131] Zhang Z, Deng W and Jiang C 2021 A PDF-based performance shift approach for reliability-based design optimization *Comput. Methods Appl. Mech. Eng.* **374** 113610
[132] Huang B and Du X 2006 A robust design method using variable transformation and Gauss-Hermite integration *Int. J. Numer. Methods Eng.* **66** 1841–58
[133] Lee D and Rahman S 2021 Robust design optimization under dependent random variables by a generalized polynomial chaos expansion *Struct. Multidiscip. Optim.* **63** 2425–57
[134] Feng R, Elghazouli A Y, Li Y, Dong Y and Wang Z 2025 Life-cycle seismic resilience of deteriorating highway bridges under mainshock-aftershock sequences *Bull. Earthq. Eng.* **23** 2137–69
[135] Li Z, Zhang Z and Wang T 2024 Wind fragility analysis of UHV double column suspended guyed tower considering multiple performance levels *Proc. Chin. Soc. Electr. Eng.* **44** 8304–15
[136] Wang T, Zhang Z, Li Z, Lu D and Tan Y 2025 Wind disaster risk assessment of UHV double column suspended guyed tower *Proc. Chin. Soc. Electr. Eng.* **45** 6140–52
[137] Forsberg S, Göteman M, Thomas K and Bergkvist M 2024 Resilience to extreme storm conditions: a comparative study of two power systems with varying dependencies on offshore wind *Results Eng.* **23** 102408



Tao Wang is currently a Post-Doctoral Fellow with the Department of Civil and Environmental Engineering, The Hong Kong Polytechnic University, China. His current research interests include uncertainty quantification, structural and system reliability, wind-induced risk and resilience assessment of power transmission structures and amphibious robots for power facility maintenance.



Da-Gang Lu is a professor with the School of Civil Engineering, Harbin Institute of Technology, China. His current research interests include structural reliability, seismic fragility, analysis of multi-disaster safety, risk and resilience in civil engineering, as well as seismic design methods.



You Dong is an associate professor with the Department of Civil and Environmental Engineering, The Hong Kong Polytechnic University, China. His current research interests include life-cycle performance, intelligent maintenance and resilience assessment of infrastructure, climate change adaptation, and the application of AI in civil engineering.



Dan M Frangopol is a Fazlur R. Khan chair professor with the Department of Civil and Environmental Engineering, Lehigh University, USA. His current research interests include structural reliability, life-cycle management of engineering structures, multi-disaster risk analysis, and theories and engineering applications of infrastructure resilience.



Yi-Qiu Tan is a professor with the School of Transportation Science and Engineering, Harbin Institute of Technology, China. Her current research interests include the durability and safety of asphalt roads in cold regions, prevention of ice and snow disasters, integrated design method of structure and material, and intelligent maintenance of transportation infrastructure.